MATHEMATICS OF COMPUTATION
Volume 92, Number 340, March 2023, Pages 557–582
https://doi.org/10.1090/mcom/3790
Article electronically published on October 13, 2022

ANALYSIS OF DIVERGENCE-FREE H^1 CONFORMING FEM WITH IMEX-SAV SCHEME FOR THE NAVIER-STOKES EQUATIONS AT HIGH REYNOLDS NUMBER

YONGBIN HAN, YANREN HOU, AND MIN ZHANG

ABSTRACT. In this paper, we analyze the first-order implicit-explicit type scheme based on the scalar auxiliary variable (SAV) with divergence-free H^1 conforming finite element method (FEM) in space for the evolutionary incompressible Navier-Stokes equations at high Reynolds number. The stability and a priori error estimates are given, in which the constants are independent of the Reynolds number. The velocity energy estimate is given without any condition on the time step, however, the a priori error estimates for the velocity are obtained with severe time step restrictions. In addition, a Reynolds-dependent error bound with convergence order of $k+1$ in space is also obtained for the velocity error in the L^2 norm with no time step restrictions. Here, k is the polynomial order of the velocity space. Some numerical experiments are carried out to verify the analytical results.

1. INTRODUCTION

As we know, a large number of works have been devoted to construct efficient and stable numerical methods for solving the evolutionary Navier-Stokes equations [15, 16, 26], in which the velocity and the pressure are often coupled together by the incompressibility constraint. A coupled approach often requires solving a saddle point problem at each time step, which makes it difficult to solve numerically. It is highly desirable to be implicit with respect to the linear Stokes terms and explicit with respect to the nonlinear terms, so that we only need to solve the linear Stokes problem with constant coefficients at each time step. Thus, the setup of linear systems and solvers or preconditioners can be done once and reused at each time step. Further, if a decoupled method can be used to solve the Stokes problem, such that we only need to solve a series of Poisson-type equations, it will be more efficient.

However, the completely explicit treatment of the nonlinear terms would introduce severe time step restrictions to obtain the energy stability. Recently, the developed method [20] based on the IMEX-scalar auxiliary variable (SAV) scheme with the spectral method in space for the Navier-Stokes equations is unconditionally energy stable without any condition on the time step. It is decoupled and only needs to solve a sequence of Poisson-type equations. Subsequently, the IMEX-SAV

Received by the editor January 19, 2022, and, in revised form, July 14, 2022, and August 8, 2022.

2020 *Mathematics Subject Classification.* Primary 65M60, 65M12, 35Q30.

Key words and phrases. Reynolds-robust, divergence-free H^1 conforming FEM, IMEX-SAV time-marching, evolutionary Navier-Stokes equations, high Reynolds number.

This work was supported by National Natural Science Foundation of China (No. 11971378) and the Innovative Funds Plan of Henan University of Technology (No. 2021ZKCJ11).

scheme combined with the finite difference method in space was analyzed in [18]. It is proved that the velocity and pressure errors have the second-order convergence rates in time and space. Furthermore, the IMEX-SAV scheme combined with finite element method (FEM) in space has been developed for the Navier-Stokes equations in [27], in which the rigorous unconditional stability and optimal error estimates are given. However, the above IMEX-SAV schemes need to solve a nonlinear algebraic equation for the SAV, which is very difficult to show that it always has a positive solution. Later, the new SAV-pressure correction methods in [19] and the high-order IMEX-SAV schemes with Fourier-Galerkin method in space proposed in [14] are constructed, in which one only needs to solve a linear algebraic equation for the SAV. In [19], a rigorous error analysis for the first-order scheme is carried out to prove that the velocity and pressure errors are first-order accurate in time without any condition on the time step. In [14], a rigorous error analysis for the high-order IMEX-SAV schemes is carried out in a unified form, in which the time step is only required to be bounded by a constant independent of the mesh size h.

We notice that in a fully discrete formulation, the error analysis results in [14, 18, 27] are dependent on the inverse of the viscosity, which may be only applicable to the case of low Reynolds number. Recently, for the high Reynolds number problem, an enormous amount of work has proved that the constants in the velocity error bounds are independent of the inverse of the viscosity, see the recent review article [11]. And, it is well-known that the IMEX type schemes have a severe time step constraint for the high Reynolds number problem. As we can see, a variable step IMEX BDF2 method combining inf-sup stable FEM with grad-div stabilization is analyzed in [12]. It is proved that a stronger CFL condition is needed, which relaxes the CFL condition in [9] for the high Reynolds number problem. However, so far there is no strict error analysis for the IMEX-SAV schemes at high Reynolds number. We were motivated by the question that in view of the fact that the IMEX-SAV schemes are unconditionally energy stable, whether they have the Reynolds-robust error bounds for the velocity without any condition on the time step for the high Reynolds number problem. In this paper, we consider a divergence-free H^1 conforming FEM in space combined with the IMEX-SAV scheme proposed in [19] for the Navier-Stokes equations. Notice that the divergence-free H^1 conforming FEM to approach the evolutionary Navier-Stokes equations was analyzed in a space semidiscretization formulation, where the error estimates for the velocity are independent of both the Reynolds number and the pressure [24].

In this paper, we analyze the divergence-free H^1 conforming FEM with the first-order IMEX-SAV scheme for the Navier-Stokes equations at high Reynolds number. The stability and a priori error estimates are given, in which the constants are independent of the negative powers of the viscosity. The velocity energy estimate is obtained with no time step restrictions, however, the a priori error estimates for the velocity are given under the CFL condition of the form $\Delta t \leq Ch^2$. As we can see, error analysis of the IMEX-SAV methods in the literature stresses that the error bounds are obtained with almost no time step restrictions. However, a careful review of the proofs of those error bounds reveals that they depend strongly on the Reynolds number. To the best of our knowledge, it might be the first time in the literature to prove that the IMEX-SAV type schemes have the Reynolds-robust error bound $O(h^k + \Delta t)$ of the velocity under the CFL condition for the Navier-Stokes equations at high Reynolds number.

In addition, readers should not be misled to think that this is a worse method than those previously published in the literature where errors bounds are obtained with almost no time step restrictions. To avoid this, we continue to complete the error analysis with the error bounds obtained with no time step restrictions similar to that in [19] for the two-dimensional case, in which the error constants are dependent on the negative powers of the viscosity. We obtain the Reynolds-dependent error bound $O(h^{k+1}+\Delta t)$ for the velocity L^2 error. Notice that the error analysis results in [27] are suboptimal with convergence order of k in space. Furthermore, we also give some comments on the three-dimensional case. Finally, we carry out some numerical experiments to demonstrate our analytical results.

The outline of the paper is as follows: In Section 2, we present some preliminaries and notations. In Section 3, we present the divergence-free H^1 conforming FEM with the first-order IMEX-SAV scheme and give the unconditional energy stability estimate. In Section 4, we carry out a rigorous error analysis for the velocity. Numerical experiments are presented in Section 5 to validate our theoretical results.

2. Preliminaries and notations

Consider a domain D, the Sobolev spaces $W^{j,p}(D)$ for scalar-valued functions are defined with associated norms $\|\cdot\|_{W^{j,p}(D)}$ and seminorms $|\cdot|_{W^{j,p}(D)}$ for $j\geqslant 0$ and $p\geqslant 1$. When $j=0$, $W^{0,p}(D)=L^p(D)$, and when $j=2$, $W^{j,2}(D)=H^j(D)$. For simplicity, $\|\cdot\|_{W^{j,p}(\Omega)}$ is used to denote the norm both in $W^{j,p}(\Omega)$ and in $\left[W^{j,p}(\Omega)\right]^d$. We use $\|\cdot\|_j$ (resp. $|\cdot|_j$) to denote the norm (resp. seminorm) both in $H^j(\Omega)$ and in $\left[H^j(\Omega)\right]^d$. We use $\|\cdot\|_{L^p}$ to denote the norm both in $L^p(\Omega)$ and in $\left[L^p(\Omega)\right]^d$. The inner product and norm of $L^2(\Omega)$ or $\left[L^2(\Omega)\right]^d$ will be denoted by $(\cdot,\cdot)$ and $\|\cdot\|$, respectively. The norm of the dual space $H^{-1}(\Omega)$ of $H_0^1(\Omega)$ is denoted by $\|\cdot\|_{-1}$. The exact meaning will be clear by the context. Vector- and tensor-valued functions or spaces will be indicated with bold letters. In addition, introduce the Bochner space $L^p(0,T;Y)(1\leq p\leq\infty)$, where Y is a Banach space. $\|v\|_{\mathcal{L}^p(0,T;Y)}$ represents a discrete approximation of $\|v\|_{L^p(0,T;Y)}$.

Assume that $\mathit{\Omega}\subset\mathbb{R}^d$ $(d=2,3)$, is a bounded convex polygonal or polyhedral domain. We consider the following incompressible Navier-Stokes equations:

$$
\begin{cases}
\partial_t\boldsymbol{u}-\nu\Delta\boldsymbol{u}+(\boldsymbol{u}\cdot\nabla)\boldsymbol{u}+\nabla p=\boldsymbol{f}, & (0,T]\times\mathit{\Omega},\\
\nabla\cdot\boldsymbol{u}=0, & (0,T]\times\mathit{\Omega},\\
\boldsymbol{u}=\boldsymbol{0}, & (0,T]\times\partial\mathit{\Omega},\\
\boldsymbol{u}(0,\boldsymbol{x})=\boldsymbol{u}_0(\boldsymbol{x}), & \mathit{\Omega},
\end{cases}
\tag{1}
$$

where $\boldsymbol{u}$ is the velocity field, p the kinematic pressure, $\nu>0$ the kinematic viscosity, $\boldsymbol{u}_0$ an initial velocity and $\boldsymbol{f}$ represents the external body force. We introduce the following spaces

$$\boldsymbol{V}=\boldsymbol{H}_0^1(\Omega),\ Q=L_0^2(\Omega)=\{q\in L^2(\Omega),\int_\Omega q\,dx=0\}.$$

The weak formulation of (1) can be written as follows: find $(\boldsymbol{u},p):(0,T]\to(\boldsymbol{V},Q)$, such that

$$
\begin{aligned}
(\partial_t\boldsymbol{u},\boldsymbol{v})+\nu a(\boldsymbol{u},\boldsymbol{v})+c(\boldsymbol{u},\boldsymbol{u},\boldsymbol{v})+b(\boldsymbol{v},p)&=(\boldsymbol{f},\boldsymbol{v}), && \forall\boldsymbol{v}\in\boldsymbol{V},\\
b(\boldsymbol{u},q)&=0, && \forall q\in Q.
\end{aligned}
\tag{2}
$$

Here, the multilinear forms are defined by

$$a(\boldsymbol{u},\boldsymbol{v}) = \int_\Omega \nabla\boldsymbol{u}:\nabla\boldsymbol{v}\,\mathrm{d}\boldsymbol{x}, \quad c(\boldsymbol{u},\boldsymbol{u},\boldsymbol{v}) = \int_\Omega (\boldsymbol{u}\cdot\nabla)\boldsymbol{u}\cdot\boldsymbol{v}\,\mathrm{d}\boldsymbol{x},$$

$$b(\boldsymbol{u},q) = -\int_\Omega q(\nabla\cdot\boldsymbol{u})\,\mathrm{d}\boldsymbol{x}.$$

The weakly divergence-free space is denoted by $\boldsymbol{V}^{\mathrm{div}} = \{\boldsymbol{v}\in\boldsymbol{V} : \nabla\cdot\boldsymbol{v} = 0\}$.

Let $\mathcal{T}_h$ be a shape-regular and quasi-uniform simplicial mesh of Ω with mesh size $h = \max_{K\in\mathcal{T}_h} h_K$, where h_K denotes the diameter of the element $K\in\mathcal{T}_h$. We consider the Scott-Vogelius pair of order $k\in\mathbb{N}$ for the velocity and the pressure, as follows:

$$\boldsymbol{V}_h = [\mathbb{P}_k]^d \cap \boldsymbol{V}, \quad Q_h = \mathbb{P}_{k-1}^{\mathrm{disc}} \cap Q,$$

with

$$\mathbb{P}_k = \{v_h \in C(\bar{\Omega}) : v_h|_K \in P_k(K), \forall K\in\mathcal{T}_h\},$$
$$\mathbb{P}_{k-1}^{\mathrm{disc}} = \{q_h \in L^2(\Omega) : q_h|_K \in P_{k-1}(K), \forall K\in\mathcal{T}_h\},$$

where $P_l(D)$ denotes the space of polynomials of degree $l>0$ on a domain D. The spaces $\boldsymbol{V}_h$ and Q_h form an inf-sup stable FE pair on meshes without singular vertices for $k\geqslant 4$ $(d=2)$ and $k\geqslant 6$ $(d=3)$, and on barycenter-refined meshes for $k\geqslant d$, see [2, 4, 13, 25]. Namely, there exists $\beta>0$, independent of the mesh size h, such that

$$\inf_{q_h\in Q_h\setminus\{0\}} \sup_{\boldsymbol{v}_h\in\boldsymbol{V}_h\setminus\{\boldsymbol{0}\}} \frac{b(\boldsymbol{v}_h,q_h)}{|\boldsymbol{v}_h|_1\|q_h\|_{L^2}} \geqslant \beta. \tag{3}$$

The global spaces $\boldsymbol{V}_h$ and Q_h are divergence-conforming, namely, $\nabla\cdot\boldsymbol{V}_h \subseteq Q_h$. Introduce the exactly divergence-free space

$$\boldsymbol{V}_h^{\mathrm{div}} = \{\boldsymbol{v}_h\in\boldsymbol{V}_h : b(\boldsymbol{v}_h,q_h)=0,\ \forall q_h\in Q_h\}.$$

We will use the Poincaré-Friedrichs inequality

$$\|\boldsymbol{v}\| \le C\|\nabla\boldsymbol{v}\|, \quad \forall v\in \boldsymbol{H}_0^1(\Omega).$$

Notice

$$c(\boldsymbol{u},\boldsymbol{v},\boldsymbol{w}) = -c(\boldsymbol{u},\boldsymbol{w},\boldsymbol{v}), \quad \forall\boldsymbol{v},\boldsymbol{w}\in\boldsymbol{V}, \forall\boldsymbol{u}\in\boldsymbol{V}^{\mathrm{div}},$$

therefore $c(\boldsymbol{u},\boldsymbol{w},\boldsymbol{w})=0$, $\forall\boldsymbol{w}\in\boldsymbol{V},\forall\boldsymbol{u}\in\boldsymbol{V}^{\mathrm{div}}$. Let $\boldsymbol{u}\in\boldsymbol{V}^{\mathrm{div}},\boldsymbol{v},\boldsymbol{w}\in\boldsymbol{V}$, then for $d=2$, it holds [3]

$$c(\boldsymbol{u},\boldsymbol{v},\boldsymbol{w}) \le C\|\boldsymbol{u}\|^{\frac12}\|\nabla\boldsymbol{u}\|^{\frac12}\|\nabla\boldsymbol{v}\|\|\boldsymbol{w}\|^{\frac12}\|\nabla\boldsymbol{w}\|^{\frac12}. \tag{4}$$

Define the discrete Stokes operator $A_h : \boldsymbol{V}_h^{\mathrm{div}} \to \boldsymbol{V}_h^{\mathrm{div}}$:

$$(A_h\boldsymbol{v}_h,\boldsymbol{w}_h) = (\nabla\boldsymbol{v}_h,\nabla\boldsymbol{w}_h), \quad \forall\boldsymbol{v}_h,\boldsymbol{w}_h\in\boldsymbol{V}_h^{\mathrm{div}}.$$

It is symmetric and positive definite, see [15, 24]. Note that from the definition, it follows that for $\forall\boldsymbol{v}_h\in\boldsymbol{V}_h^{\mathrm{div}}$,

(5)

$$\|(A_h)^{1/2}\boldsymbol{v}_h\| = \|\nabla\boldsymbol{v}_h\|, \quad \|\nabla(A_h)^{-1/2}\boldsymbol{v}_h\| = \|\boldsymbol{v}_h\|, \quad \|\nabla(A_h)^{-1}\boldsymbol{v}_h\| = \|(A_h)^{-1/2}\boldsymbol{v}_h\|.$$

Let $I_h\boldsymbol{u}\in\boldsymbol{V}_h$ be the Lagrange interpolant of a continuous function $\boldsymbol{u}$. The following bound can be found in [4, Theorem 4.4.4]

$$|\boldsymbol{u}-I_h\boldsymbol{u}|_{W^{m,p}(K)} \le c_{\mathrm{int}} h_K^{n-m}|\boldsymbol{u}|_{W^{n,p}(K)}, \quad 0\le m\le n\le k+1, \tag{6}$$

where $n > d/p$ when $1 < p \leq \infty$, and $n \geq d$ when $p = 1$. Let $P^l w$ denote the L^2-projection of w onto Q_h, then there exists C, independent of h such that for $0 \leq j \leq s \leq l+1$, $1 \leq p \leq \infty$ [10, Theorem 1.45],

$$|w - P^l w|_{W^{j,p}(\Omega)} \leq Ch^{s-j}|w|_{W^{s,p}(\Omega)}, \quad \forall w \in W^{s,p}(\Omega) \cap Q. \tag{7}$$

We have the following inverse inequality such that for $0 \leq n \leq m \leq 1, 1 \leq q \leq p \leq \infty$ [6, Theorem 3.2.6],

$$\|\boldsymbol{v}_h\|_{W^{m,p}(K)} \leq C_{\text{inv}} h_K^{n-m-d(\frac{1}{q}-\frac{1}{p})} \|\boldsymbol{v}_h\|_{W^{n,q}(K)}, \quad \forall v_h \in \boldsymbol{V}_h. \tag{8}$$

We use the following Sobolev's embedding [1]: For $1 \leq p < d/s$, let q be such that $\frac{1}{q} = \frac{1}{p} - \frac{s}{d}$. There exists a constant C such that

$$\|v\|_{L^{q'}(\Omega)} \leq C\|v\|_{W^{s,p}(\Omega)}, \quad \frac{1}{q'} \geq \frac{1}{q}, \quad \forall v \in W^{s,p}(\Omega).$$

If $p > d/s$, the above inequality is valid for $q' = \infty$.

For the following analysis, the discrete Stokes projection will be used to split the velocity error [24]. The following Stokes problem is given by

$$\begin{cases} -\nu\Delta \boldsymbol{u}_s + \nabla p_s = \boldsymbol{g}, & \Omega, \\ \nabla \cdot \boldsymbol{u}_s = 0, & \Omega, \\ \boldsymbol{u}_s = \boldsymbol{0}, & \partial\Omega, \end{cases} \tag{9}$$

with $\boldsymbol{g} = \boldsymbol{f} - \partial_t \boldsymbol{u} - (\boldsymbol{u} \cdot \nabla)\boldsymbol{u} - \nabla p = -\nu\Delta\boldsymbol{u}$, in which $(\boldsymbol{u}, p)$ is the solution of (1) with $\boldsymbol{u} \in \boldsymbol{V} \cap \boldsymbol{H}^{k+1}(\Omega)$ and $p \in Q \cap H^k(\Omega) (k \geq 1)$, thus, the pair $(\boldsymbol{u}, 0)$ is the solution of (9). The Scott-Vogelius FEM reads as follows: find $(\boldsymbol{u}_{sh}, p_{sh}) \in \boldsymbol{V}_h \times Q_h$ such that for $\forall(\boldsymbol{v}_h, q_h) \in \boldsymbol{V}_h \times Q_h$,

$$\nu a(\boldsymbol{u}_{sh}, \boldsymbol{v}_h) + b(\boldsymbol{v}_h, p_{sh}) + b(\boldsymbol{u}_{sh}, q_h) = (\boldsymbol{g}, \boldsymbol{v}_h).$$

Then, $\boldsymbol{u}_{sh}$ is defined as the discrete Stokes projection $\boldsymbol{\pi}_s \boldsymbol{u}$ of $\boldsymbol{u}$, which is exactly divergence-free. It is straightforward that $a(\boldsymbol{u} - \boldsymbol{\pi}_s\boldsymbol{u}, \boldsymbol{v}_h) = 0, \forall \boldsymbol{v}_h \in \boldsymbol{V}_h^{\text{div}}$. We have the following estimate [11, 24]:

$$\|\boldsymbol{u} - \boldsymbol{\pi}_s\boldsymbol{u}\|_{L^2} + h|\boldsymbol{u} - \boldsymbol{\pi}_s\boldsymbol{u}|_1 \leq C_s h \inf_{\boldsymbol{v}_h \in \boldsymbol{V}_h} \|\boldsymbol{u} - \boldsymbol{v}_h\|_1. \tag{10}$$

In addition, the following maximum norm estimates hold [5]:

$$\|\boldsymbol{u} - \boldsymbol{\pi}_s\boldsymbol{u}\|_{L^\infty} \leq C_\infty h \left(\ln \frac{1}{h}\right) |\boldsymbol{u}|_{W^{1,\infty}}, \tag{11}$$

$$|\boldsymbol{\pi}_s\boldsymbol{u}|_{W^{1,\infty}} \leq C_\infty |\boldsymbol{u}|_{W^{1,\infty}}, \tag{12}$$

where C_∞ does not depend on ν. Assume that the solution $(\boldsymbol{u}, p)$ of (1) is sufficiently smooth in time such that we can take $\boldsymbol{g} = \partial_t(-\nu\Delta\boldsymbol{u})$ in (9). Then, we have

$$\|\partial_t(\boldsymbol{u} - \boldsymbol{\pi}_s\boldsymbol{u})\|_{L^2} + h|\partial_t(\boldsymbol{u} - \boldsymbol{\pi}_s\boldsymbol{u})|_1 \leq Ch \inf_{\boldsymbol{v}_h \in V_h} \|\partial_t\boldsymbol{u} - \boldsymbol{v}_h\|_1. \tag{13}$$

Introduce the following two essential lemmas, which are frequently used in fully discrete analysis of the Navier-Stokes equations.

Lemma 2.1 ([15, Lemma A.56]). *Let $\Delta t, B, a_n, b_n, c_n$ be non-negative numbers such that*

$$a_{N+1} + \Delta t \sum_{n=0}^{N+1} b_n \leq B + \Delta t \sum_{n=0}^{N+1} c_n + \Delta t \sum_{n=0}^{N} \gamma_n a_n, \quad \textit{for } N \geq 0,$$

is given, then it holds

$$a_{N+1} + \Delta t \sum_{n=0}^{N+1} b_n \leq \exp(\Delta t \sum_{n=0}^{N} \gamma_n)(B + \Delta t \sum_{n=0}^{N+1} c_n), \qquad \textit{for } N \geq 0.$$

Lemma 2.2 ([15, Lemma 7.67])**.** *Let $v, \partial_t v, \partial_{tt} v \in L^2(t^n, t^{n+1}; L^2(\Omega))$, then*

$$\|\partial_t v^{n+1} - \frac{v^{n+1} - v^n}{\Delta t}\|^2_{L^2(\Omega)} \leq \Delta t \|\partial_{tt} v\|^2_{L^2(t^n, t^{n+1}; L^2(\Omega))}. \tag{14}$$

3. The IMEX-SAV scheme

In this section, we present the divergence-free H^1 conforming FEM with the IMEX-SAV scheme based on the SAV-pressure correction method in [19] for the Navier-Stokes equations. Nevertheless, it is noted that the following analytical ideas are quite different from that in [19].

Firstly, the Navier-Stokes equations can be rewritten into the following equivalent system:

$$\begin{aligned} \partial_t \boldsymbol{u} + \frac{q(t)}{\exp(-\frac{t}{T})} \boldsymbol{u} \cdot \nabla \boldsymbol{u} - \nu \Delta \boldsymbol{u} + \nabla p = \boldsymbol{f}&, \\ \nabla \cdot \boldsymbol{u} = 0&, \end{aligned} \tag{15}$$

and

$$\frac{dq(t)}{dt} = -\frac{1}{T} q(t) + \frac{1}{\exp(-\frac{t}{T})} c(\boldsymbol{u}, \boldsymbol{u}, \boldsymbol{u}), \tag{16}$$

with the scalar auxiliary variable $q(t) = \exp(-\frac{t}{T})$, see [19]. We consider a uniform partition of the time interval $[0, T]$ with step-size Δt. Set $\Delta t = T/(N+1), t^n = n\Delta t$, $0 \leq n \leq N+1$. Let $\boldsymbol{u}_h^0$ be an approximation of $\boldsymbol{u}_0$ and $q^0 = 1$. The IMEX-SAV scheme can be written as follows: find $(\boldsymbol{u}_h^{n+1}, p_h^{n+1}, q^{n+1})$ such that for $\forall (\boldsymbol{v}_h, q_h) \in \boldsymbol{V}_h \times Q_h$,

$$\begin{aligned} (\frac{\boldsymbol{u}_h^{n+1} - \boldsymbol{u}_h^n}{\Delta t}, \boldsymbol{v}_h) + \nu a(\boldsymbol{u}_h^{n+1}, \boldsymbol{v}_h) + b(\boldsymbol{v}_h, p_h^{n+1}) + \frac{q^{n+1}}{\exp(-\frac{t^{n+1}}{T})} c(\boldsymbol{u}_h^n, \boldsymbol{u}_h^n, \boldsymbol{v}_h) = (\boldsymbol{f}^{n+1}, \boldsymbol{v}_h)&, \\ b(\boldsymbol{u}_h^{n+1}, q_h) = 0&, \end{aligned} \tag{17}$$

and

$$\frac{q^{n+1} - q^n}{\Delta t} = -\frac{1}{T} q^{n+1} + \frac{1}{\exp(-\frac{t^{n+1}}{T})} c(\boldsymbol{u}_h^n, \boldsymbol{u}_h^n, \boldsymbol{u}_h^{n+1}). \tag{18}$$

Now, by similarly following [19], we show how to solve (17)-(18) efficiently. Set

$$\begin{aligned} \boldsymbol{u}_h^{n+1} &= \boldsymbol{u}_{1,h}^{n+1} + W^{n+1} \boldsymbol{u}_{2,h}^{n+1}, \\ p_h^{n+1} &= p_{1,h}^{n+1} + W^{n+1} p_{2,h}^{n+1}, \end{aligned} \tag{19}$$

with $W^{n+1} = \exp(\frac{t^{n+1}}{T}) q^{n+1}$. We can insert (19) in (17) to obtain

$$\begin{aligned} (\frac{\boldsymbol{u}_{1,h}^{n+1} - \boldsymbol{u}_h^n}{\Delta t}, \boldsymbol{v}_h) + \nu a(\boldsymbol{u}_{1,h}^{n+1}, \boldsymbol{v}_h) + b(\boldsymbol{v}_h, p_{1,h}^{n+1}) = (\boldsymbol{f}^{n+1}, \boldsymbol{v}_h), &\quad \forall \boldsymbol{v}_h \in \boldsymbol{V}_h, \\ b(\boldsymbol{u}_{1,h}^{n+1}, q_h) = 0, &\quad \forall q_h \in Q_h, \end{aligned} \tag{20}$$

and

$$(21)\qquad \begin{aligned}(\frac{\boldsymbol{u}_{2,h}^{n+1}}{\Delta t},\boldsymbol{v}_h)+\nu a(\boldsymbol{u}_{2,h}^{n+1},\boldsymbol{v}_h)+b(\boldsymbol{v}_h,p_{2,h}^{n+1})+c(\boldsymbol{u}_h^n,\boldsymbol{u}_h^n,\boldsymbol{v}_h)=0,\quad \forall \boldsymbol{v}_h\in \boldsymbol{V}_h,\\ b(\boldsymbol{u}_{2,h}^{n+1},q_h)=0,\quad \forall q_h\in Q_h.\end{aligned}$$

Once $\boldsymbol{u}_{i,h}^{n+1}$ and $p_{i,h}^{n+1}$ $(i=1,2)$ are solved, we can obtain W^{n+1} from (18) by

$$\begin{aligned}&\left(\frac{T+\Delta t}{T\Delta t}-\exp(\frac{2t^{n+1}}{T})c(\boldsymbol{u}_h^n,\boldsymbol{u}_h^n,\boldsymbol{u}_{2,h}^{n+1})\right)\exp(-\frac{t^{n+1}}{T})W^{n+1}\\ &=\exp(\frac{t^{n+1}}{T})c(\boldsymbol{u}_h^n,\boldsymbol{u}_h^n,\boldsymbol{u}_{1,h}^{n+1})+\frac{1}{\Delta t}q^n.\end{aligned}$$

Thus, $\boldsymbol{u}_h^{n+1}$ and p_h^{n+1} can be obtained from (19). In addition, the high-order IMEX-BDF SAV schemes in time can be similarly constructed.

We notice that at each time step, (20) and (21) can be solved by the iterative penalty method, see [4, Chapter 13] and [21]. Thus, we only need to solve a series of positive-definite Poisson-type problems with constant coefficients.

Next, the velocity energy estimate is given without any condition on the time step, in which the constants are independent of the negative powers of the viscosity.

Lemma 3.1. *Let $\boldsymbol{f}\in L^2(0,T;\boldsymbol{L}^2(\Omega))$, $\boldsymbol{u}_0\in \boldsymbol{L}^2(\Omega)$, and $\boldsymbol{u}_h^0$ is an approximation of $\boldsymbol{u}_0$. Then, we have the following stability estimate: for $0\le n\le N$,*

$$(22)\qquad \begin{aligned}&\frac12\|\boldsymbol{u}_h^{n+1}\|_{L^2}^2+\sum_{j=1}^{n+1}\frac14\|\boldsymbol{u}_h^j-\boldsymbol{u}_h^{j-1}\|_{L^2}^2+\frac12|q^{n+1}|^2+\sum_{j=1}^{n+1}\frac12|q^j-q^{j-1}|^2\\ &+\sum_{j=1}^{n+1}\frac1T\Delta t|q^j|^2+\nu\Delta t\sum_{j=1}^{n+1}|\boldsymbol{u}_h^j|_1^2\\ &\le \exp(1)(\frac12\|\boldsymbol{u}_h^0\|_{L^2}^2+\frac12|q^0|^2+\frac32 T\Delta t\sum_{j=1}^{n+1}\|\boldsymbol{f}^j\|_{L^2}^2).\end{aligned}$$

Proof. Firstly, taking $(\boldsymbol{v}_h,q_h)=(\boldsymbol{u}_h^{n+1},p_h^{n+1})$ in (17) yields

$$(23)\qquad (\frac{\boldsymbol{u}_h^{n+1}-\boldsymbol{u}_h^n}{\Delta t},\boldsymbol{u}_h^{n+1})+\nu a(\boldsymbol{u}_h^{n+1},\boldsymbol{u}_h^{n+1})+\frac{q^{n+1}}{\exp(-\frac{t^{n+1}}{T})}c(\boldsymbol{u}_h^n,\boldsymbol{u}_h^n,\boldsymbol{u}_h^{n+1})=(\boldsymbol{f}^{n+1},\boldsymbol{u}_h^{n+1}).$$

Due to

$$(24)\qquad (\boldsymbol{u}_h^{n+1}-\boldsymbol{u}_h^n,\boldsymbol{u}_h^{n+1})=\frac12(\|\boldsymbol{u}_h^{n+1}\|_{L^2}^2+\|\boldsymbol{u}_h^{n+1}-\boldsymbol{u}_h^n\|_{L^2}^2-\|\boldsymbol{u}_h^n\|_{L^2}^2).$$

Inserting (24) in (23), we can get

$$(25)\qquad \begin{aligned}&\frac12\|\boldsymbol{u}_h^{n+1}\|_{L^2}^2+\frac12\|\boldsymbol{u}_h^{n+1}-\boldsymbol{u}_h^n\|_{L^2}^2+\nu\Delta t|\boldsymbol{u}_h^{n+1}|_1^2+\Delta t\frac{q^{n+1}}{\exp(-\frac{t^{n+1}}{T})}c(\boldsymbol{u}_h^n,\boldsymbol{u}_h^n,\boldsymbol{u}_h^{n+1})\\ &=\frac12\|\boldsymbol{u}_h^n\|_{L^2}^2+\Delta t(\boldsymbol{f}^{n+1},\boldsymbol{u}_h^{n+1}).\end{aligned}$$

Multiplying (18) by $q^{n+1}\Delta t$, we have

$$(26)\qquad \frac12|q^{n+1}|^2-\frac12|q^n|^2+\frac12|q^{n+1}-q^n|^2=-\frac1T\Delta t|q^{n+1}|^2+\Delta t\frac{q^{n+1}}{\exp(-\frac{t^{n+1}}{T})}c(\boldsymbol{u}_h^n,\boldsymbol{u}_h^n,\boldsymbol{u}_h^{n+1}).$$

Combining (25) and (26), we can obtain

(27)

$$\begin{aligned}
&\frac{1}{2}\|\boldsymbol{u}_h^{n+1}\|_{L^2}^2+\sum_{j=1}^{n+1}\frac{1}{2}\|\boldsymbol{u}_h^j-\boldsymbol{u}_h^{j-1}\|_{L^2}^2+\frac{1}{2}|q^{n+1}|^2+\sum_{j=1}^{n+1}\frac{1}{2}|q^j-q^{j-1}|^2\\
&\quad+\sum_{j=1}^{n+1}\frac{1}{T}\Delta t|q^j|^2+\nu\Delta t\sum_{j=1}^{n+1}|\boldsymbol{u}_h^j|_1^2\\
&\leq\frac{1}{2}\|\boldsymbol{u}_h^0\|_{L^2}^2+\frac{1}{2}|q^0|^2+\sum_{j=1}^{n+1}\Delta t(\boldsymbol{f}^j,\boldsymbol{u}_h^j-\boldsymbol{u}_h^{j-1})+\sum_{j=1}^{n+1}\Delta t(\boldsymbol{f}^j,\boldsymbol{u}_h^{j-1})\\
&\leq\frac{1}{2}\|\boldsymbol{u}_h^0\|_{L^2}^2+\frac{1}{2}|q^0|^2+\sum_{j=1}^{n+1}(\Delta t)^2\|\boldsymbol{f}^j\|_{L^2}^2+\frac{1}{2}T\Delta t\sum_{j=1}^{n+1}\|\boldsymbol{f}^j\|_{L^2}^2\\
&\quad+\sum_{j=1}^{n+1}\frac{1}{4}\|\boldsymbol{u}_h^j-\boldsymbol{u}_h^{j-1}\|_{L^2}^2+\sum_{j=0}^{n}\frac{\Delta t}{T}\frac{1}{2}\|\boldsymbol{u}_h^j\|_{L^2}^2\\
&\leq\frac{1}{2}\|\boldsymbol{u}_h^0\|_{L^2}^2+\frac{1}{2}|q^0|^2+\frac{3}{2}T\Delta t\sum_{j=1}^{n+1}\|\boldsymbol{f}^j\|_{L^2}^2+\sum_{j=1}^{n+1}\frac{1}{4}\|\boldsymbol{u}_h^j-\boldsymbol{u}_h^{j-1}\|_{L^2}^2+\sum_{j=0}^{n}\frac{\Delta t}{T}\frac{1}{2}\|\boldsymbol{u}_h^j\|_{L^2}^2.
\end{aligned}$$

Then, using Lemma 2.1, we can finish the proof. □

Remark 3.2. In the absence of the external force $\boldsymbol{f}$, from the first inequality of (27), we have the following energy estimate: for $0\leq n\leq N$,

$$\begin{aligned}
&\frac{1}{2}\|\boldsymbol{u}_h^{n+1}\|_{L^2}^2+\sum_{j=1}^{n+1}\frac{1}{2}\|\boldsymbol{u}_h^j-\boldsymbol{u}_h^{j-1}\|_{L^2}^2+\frac{1}{2}|q^{n+1}|^2+\sum_{j=1}^{n+1}\frac{1}{2}|q^j-q^{j-1}|^2\\
&\quad+\sum_{j=1}^{n+1}\frac{1}{T}\Delta t|q^j|^2+\nu\Delta t\sum_{j=1}^{n+1}|\boldsymbol{u}_h^j|_1^2\leq\frac{1}{2}\|\boldsymbol{u}_h^0\|_{L^2}^2+\frac{1}{2}|q^0|^2.
\end{aligned}$$

4. Error analysis for the velocity

In this section, we present the error estimates for the velocity in Theorems 4.1 and 4.3. Let $\left(\boldsymbol{u}_h^{n+1},p_h^{n+1},q^{n+1}\right)$ be the solution of (17)-(18) and $(\boldsymbol{u},p,q)$ be the solution of (15)-(16). Then from Lemma 3.1, we have

$$\|\boldsymbol{u}_h^m\|\leq c_0,\quad |q^m|\leq c_1,\quad \forall 0\leq m\leq N+1, \tag{28}$$

where the constants c_i $(i=0,1)$ are independent of h and ν^{-1}. Assume $\boldsymbol{u}\in L^\infty\left(0,T;\boldsymbol{W}^{1,\infty}(\Omega)\right)$, then we have

$$\|\boldsymbol{u}^m\|_{1,\infty}\leq C,\ \forall 0\leq m\leq N+1. \tag{29}$$

In the following error analysis, we will frequently use (28) and (29). We set

$$\begin{aligned}
\boldsymbol{u}^n-\boldsymbol{u}_h^n&=(\boldsymbol{u}^n-\boldsymbol{\pi}_s\boldsymbol{u}^n)-(\boldsymbol{u}_h^n-\boldsymbol{\pi}_s\boldsymbol{u}^n)=\boldsymbol{\eta}^n-\boldsymbol{e}_h^n,\\
e_q^n&=q(t^n)-q^n.
\end{aligned}$$

Theorem 4.1. *Let* $\boldsymbol{u}_h^0 = \boldsymbol{\pi}_s \boldsymbol{u}_0$ *and* $q^0 = 1$*, and assume the following regularities for the velocity solution* $\boldsymbol{u}$ *of* (2)*:*

$$\begin{aligned} &\partial_{tt}\boldsymbol{u} \in L^2(0,T;\boldsymbol{H}^1(\Omega)), \quad \partial_t \boldsymbol{u} \in L^2(0,T;\boldsymbol{H}^{k+1}(\Omega)),\\ &\boldsymbol{u} \in L^\infty(0,T;\boldsymbol{H}^{k+1}(\Omega)), \quad \boldsymbol{u} \in L^\infty(0,T;\boldsymbol{W}^{1,\infty}(\Omega)). \end{aligned} \tag{30}$$

Let the time step satisfy

$$\Delta t \|\boldsymbol{u}\|^2_{L^\infty(0,T;\boldsymbol{L}^\infty(\Omega))} \le h^2. \tag{31}$$

Then, for small enough h*, there holds the following error estimate: for* $0 \le n \le N$*,*

$$\|\boldsymbol{u}^{n+1} - \boldsymbol{u}_h^{n+1}\|^2_{L^2} + |e_q^{n+1}|^2 + \nu\Delta t \sum_{j=1}^{n+1} |\boldsymbol{u}^j - \boldsymbol{u}_h^j|_1^2 \le C(\boldsymbol{u}, \partial_t\boldsymbol{u}, \partial_{tt}\boldsymbol{u}, T)(h^{2k} + (\Delta t)^2), \tag{32}$$

with a constant $C(\boldsymbol{u}, \partial_t\boldsymbol{u}, \partial_{tt}\boldsymbol{u}, T)$ *independent of* n*,* h *and* ν^{-1}*.*

Proof. The proof can be divided into Steps 1–5.

Step 1. Firstly, we have the following error equation with the test function $\boldsymbol{e}_h^{n+1} \in \boldsymbol{V}_h^{\mathrm{div}}$:

$$\begin{aligned} &(\partial_t \boldsymbol{u}^{n+1} - \frac{\boldsymbol{u}_h^{n+1} - \boldsymbol{u}_h^n}{\Delta t}, \boldsymbol{e}_h^{n+1}) + \nu a(\boldsymbol{\eta}^{n+1}, \boldsymbol{e}_h^{n+1}) - \nu a(\boldsymbol{e}_h^{n+1}, \boldsymbol{e}_h^{n+1})\\ &\quad + \frac{q(t^{n+1})}{\exp(-\frac{t^{n+1}}{T})} c(\boldsymbol{u}^{n+1}, \boldsymbol{u}^{n+1}, \boldsymbol{e}_h^{n+1}) - \frac{q^{n+1}}{\exp(-\frac{t^{n+1}}{T})} c(\boldsymbol{u}_h^n, \boldsymbol{u}_h^n, \boldsymbol{e}_h^{n+1}) = 0. \end{aligned} \tag{33}$$

We expand the left argument of the first term of (33) in the form

$$\begin{aligned} &\partial_t \boldsymbol{u}^{n+1} - \frac{\boldsymbol{u}_h^{n+1} - \boldsymbol{u}_h^n}{\Delta t}\\ &= \partial_t(\boldsymbol{u}^{n+1} - \boldsymbol{\pi}_s \boldsymbol{u}^{n+1}) + \partial_t \boldsymbol{\pi}_s \boldsymbol{u}^{n+1} - \frac{\boldsymbol{\pi}_s \boldsymbol{u}^{n+1} - \boldsymbol{\pi}_s \boldsymbol{u}^n}{\Delta t} - \frac{\boldsymbol{e}_h^{n+1} - \boldsymbol{e}_h^n}{\Delta t}. \end{aligned} \tag{34}$$

Using (34), one can obtain

$$\begin{aligned} &\frac{1}{2\Delta t}(\|\boldsymbol{e}_h^{n+1}\|^2_{L^2} + \|\boldsymbol{e}_h^{n+1} - \boldsymbol{e}_h^n\|^2_{L^2} - \|\boldsymbol{e}_h^n\|^2_{L^2}) + \nu a(\boldsymbol{e}_h^{n+1}, \boldsymbol{e}_h^{n+1})\\ &= (\partial_t(\boldsymbol{u}^{n+1} - \boldsymbol{\pi}_s \boldsymbol{u}^{n+1}), \boldsymbol{e}_h^{n+1}) + (\partial_t \boldsymbol{\pi}_s \boldsymbol{u}^{n+1} - \frac{\boldsymbol{\pi}_s \boldsymbol{u}^{n+1} - \boldsymbol{\pi}_s \boldsymbol{u}^n}{\Delta t}, \boldsymbol{e}_h^{n+1}) + \nu a(\boldsymbol{\eta}^{n+1}, \boldsymbol{e}_h^{n+1})\\ &\quad + \{\frac{q(t^{n+1})}{\exp(-\frac{t^{n+1}}{T})} c(\boldsymbol{u}^{n+1}, \boldsymbol{u}^{n+1}, \boldsymbol{e}_h^{n+1}) - \frac{q^{n+1}}{\exp(-\frac{t^{n+1}}{T})} c(\boldsymbol{u}_h^n, \boldsymbol{u}_h^n, \boldsymbol{e}_h^{n+1})\}. \end{aligned} \tag{35}$$

Next, we estimate all terms on the right-hand side of (35). For the first term on the right-hand side of (35), we have

$$\begin{aligned} (\partial_t(\boldsymbol{u}^{n+1} - \boldsymbol{\pi}_s \boldsymbol{u}^{n+1}), \boldsymbol{e}_h^{n+1}) &\le C(1+\Delta t)\|\partial_t(\boldsymbol{u}^{n+1} - \boldsymbol{\pi}_s \boldsymbol{u}^{n+1})\|^2_{L^2} + \frac{\|\boldsymbol{e}_h^{n+1} - \boldsymbol{e}_h^n\|^2_{L^2}}{16\Delta t}\\ &\quad + \|\boldsymbol{e}_h^n\|^2_{L^2}\\ &\le C\|\partial_t(\boldsymbol{u}^{n+1} - \boldsymbol{\pi}_s \boldsymbol{u}^{n+1})\|^2_{L^2} + \frac{\|\boldsymbol{e}_h^{n+1} - \boldsymbol{e}_h^n\|^2_{L^2}}{16\Delta t} + \|\boldsymbol{e}_h^n\|^2_{L^2}. \end{aligned} \tag{36}$$

Using Lemma 2.2, the commutation of temporal derivative and projection, and the stability estimate of the projection, we have

$$
\begin{aligned}
\|\partial_t \boldsymbol{\pi}_s \boldsymbol{u}^{n+1} - \frac{\boldsymbol{\pi}_s \boldsymbol{u}^{n+1} - \boldsymbol{\pi}_s \boldsymbol{u}^{n}}{\Delta t}\|^2 &\le \Delta t \|\partial_{tt} \boldsymbol{\pi}_s \boldsymbol{u}\|^2_{L^2(t^n,t^{n+1};\boldsymbol{L}^2(\Omega))} \\
&= \Delta t \|\boldsymbol{\pi}_s(\partial_{tt}\boldsymbol{u})\|^2_{L^2(t^n,t^{n+1};\boldsymbol{L}^2(\Omega))} \\
&\le C\Delta t \|\partial_{tt}\boldsymbol{u}\|^2_{L^2(t^n,t^{n+1};\boldsymbol{H}^1(\Omega))}.
\end{aligned} \tag{37}
$$

For the estimate of the second term, we use (37) to obtain

$$
\begin{aligned}
&(\partial_t \boldsymbol{\pi}_s \boldsymbol{u}^{n+1} - \frac{\boldsymbol{\pi}_s \boldsymbol{u}^{n+1} - \boldsymbol{\pi}_s \boldsymbol{u}^{n}}{\Delta t}, \boldsymbol{e}_h^{n+1}) \\
&\le C(1+\Delta t)\|\partial_t \boldsymbol{\pi}_s \boldsymbol{u}^{n+1} - \frac{\boldsymbol{\pi}_s \boldsymbol{u}^{n+1} - \boldsymbol{\pi}_s \boldsymbol{u}^{n}}{\Delta t}\|^2_{L^2} + \frac{\|\boldsymbol{e}_h^{n+1} - \boldsymbol{e}_h^n\|^2_{L^2}}{16\Delta t} + \|\boldsymbol{e}_h^n\|^2_{L^2} \\
&\le C\Delta t\|\partial_{tt}\boldsymbol{u}\|^2_{L^2(t^n,t^{n+1};\boldsymbol{H}^1(\Omega))} + \frac{\|\boldsymbol{e}_h^{n+1} - \boldsymbol{e}_h^n\|^2_{L^2}}{16\Delta t} + \|\boldsymbol{e}_h^n\|^2_{L^2}.
\end{aligned} \tag{38}
$$

For the estimate of the third term, it is straightforward that $\nu a(\boldsymbol{\eta}^{n+1}, \boldsymbol{e}_h^{n+1}) = 0$.

Step 2. We notice that in the error analysis, the most important term to deal with is the fourth term on the right-hand side of (35), which can be rewritten as follows:

$$
\begin{aligned}
&c(\boldsymbol{u}^{n+1}, \boldsymbol{u}^{n+1}, \boldsymbol{e}_h^{n+1}) - \frac{q^{n+1}}{\exp(-\frac{t^{n+1}}{T})} c(\boldsymbol{u}_h^n, \boldsymbol{u}_h^n, \boldsymbol{e}_h^{n+1}) \\
&= \underbrace{c(\boldsymbol{u}^{n+1}, \boldsymbol{u}^{n+1}, \boldsymbol{e}_h^{n+1}) - c(\boldsymbol{u}^{n}, \boldsymbol{u}^{n}, \boldsymbol{e}_h^{n+1})}_{\Theta_1} + \underbrace{c(\boldsymbol{u}^{n}, \boldsymbol{u}^{n}, \boldsymbol{e}_h^{n+1}) - c(\boldsymbol{u}_h^{n}, \boldsymbol{u}_h^{n}, \boldsymbol{e}_h^{n+1})}_{\Theta_2} \\
&\quad + \underbrace{\frac{e_q^{n+1}}{\exp(-\frac{t^{n+1}}{T})} c(\boldsymbol{u}_h^n, \boldsymbol{u}_h^n, \boldsymbol{e}_h^{n+1})}_{\Theta_3}.
\end{aligned}
$$

First, we have

$$
\begin{aligned}
&c(\boldsymbol{u}^{n+1} - \boldsymbol{u}^n, \boldsymbol{u}^{n+1}, \boldsymbol{e}_h^{n+1}) \\
&\le \frac{\|\boldsymbol{e}_h^{n+1} - \boldsymbol{e}_h^n\|^2_{L^2}}{32\Delta t} + \|\boldsymbol{e}_h^n\|^2_{L^2} + C(1+\Delta t)\|\nabla \boldsymbol{u}^{n+1}\|^2_{L^\infty}\|\boldsymbol{u}^{n+1} - \boldsymbol{u}^n\|^2_{L^2} \\
&\le \frac{\|\boldsymbol{e}_h^{n+1} - \boldsymbol{e}_h^n\|^2_{L^2}}{32\Delta t} + \|\boldsymbol{e}_h^n\|^2_{L^2} + C(1+\Delta t)\Delta t\|\nabla \boldsymbol{u}^{n+1}\|^2_{L^\infty}\|\partial_t\boldsymbol{u}\|^2_{L^2(t^n,t^{n+1};\boldsymbol{L}^2(\Omega))}.
\end{aligned} \tag{39}
$$

Then, similar to (39), we have

$$
\begin{aligned}
&c(\boldsymbol{u}^{n}, \boldsymbol{u}^{n+1} - \boldsymbol{u}^n, \boldsymbol{e}_h^{n+1}) \\
&\le \frac{\|\boldsymbol{e}_h^{n+1} - \boldsymbol{e}_h^n\|^2_{L^2}}{32\Delta t} + \|\boldsymbol{e}_h^n\|^2_{L^2} + C(1+\Delta t)\Delta t\|\boldsymbol{u}^{n}\|^2_{L^\infty}\|\partial_t\boldsymbol{u}\|^2_{L^2(t^n,t^{n+1};\boldsymbol{H}^1(\Omega))}.
\end{aligned} \tag{40}
$$

By combining (39) and (40), we can obtain

$$
\begin{aligned}
\Theta_1 &= c(\boldsymbol{u}^{n+1} - \boldsymbol{u}^n, \boldsymbol{u}^{n+1}, \boldsymbol{e}_h^{n+1}) + c(\boldsymbol{u}^{n}, \boldsymbol{u}^{n+1} - \boldsymbol{u}^n, \boldsymbol{e}_h^{n+1}) \\
&\le \frac{\|\boldsymbol{e}_h^{n+1} - \boldsymbol{e}_h^n\|^2_{L^2}}{16\Delta t} + C(\|\boldsymbol{e}_h^n\|^2_{L^2} + \Delta t\|\partial_t\boldsymbol{u}\|^2_{L^2(t^n,t^{n+1};\boldsymbol{H}^1(\Omega))}).
\end{aligned}
$$

Denote

$$\Theta_2 = \underbrace{c(\boldsymbol{u}^n,\boldsymbol{u}^n,\boldsymbol{e}_h^n) - c(\boldsymbol{u}_h^n,\boldsymbol{u}_h^n,\boldsymbol{e}_h^n)}_{\Theta_{21}} + \underbrace{c(\boldsymbol{u}^n,\boldsymbol{u}^n,\boldsymbol{e}_h^{n+1}-\boldsymbol{e}_h^n) - c(\boldsymbol{u}_h^n,\boldsymbol{u}_h^n,\boldsymbol{e}_h^{n+1}-\boldsymbol{e}_h^n)}_{\Theta_{22}}.$$

By writing $\boldsymbol{u}^n - \boldsymbol{u}_h^n = \boldsymbol{\eta}^n - \boldsymbol{e}_h^n$ and $\boldsymbol{u}_h^n = \boldsymbol{e}_h^n + \boldsymbol{u}^n - \boldsymbol{\eta}^n$, respectively, and then applying Hölder's inequality, and Young's inequality, we have

(41)

$$\begin{aligned}\Theta_{21} &= c(\boldsymbol{u}^n-\boldsymbol{u}_h^n,\boldsymbol{u}^n,\boldsymbol{e}_h^n) + c(\boldsymbol{u}_h^n,\boldsymbol{u}^n-\boldsymbol{u}_h^n,\boldsymbol{e}_h^n)\\ &= c(\boldsymbol{\eta}^n,\boldsymbol{u}^n,\boldsymbol{e}_h^n) - c(\boldsymbol{e}_h^n,\boldsymbol{u}^n,\boldsymbol{e}_h^n) + c(\boldsymbol{e}_h^n,\boldsymbol{\eta}^n,\boldsymbol{e}_h^n) + c(\boldsymbol{u}^n,\boldsymbol{\eta}^n,\boldsymbol{e}_h^n) - c(\boldsymbol{\eta}^n,\boldsymbol{\eta}^n,\boldsymbol{e}_h^n)\\ &\le \|\nabla\boldsymbol{u}^n\|_{L^\infty}\|\boldsymbol{\eta}^n\|^2 + 2\|\nabla\boldsymbol{u}^n\|_{L^\infty}\|\boldsymbol{e}_h^n\|^2 + 2\|\nabla\boldsymbol{\eta}^n\|_{L^\infty}\|\boldsymbol{e}_h^n\|^2 + \|\boldsymbol{u}^n\|_{L^\infty}\|\boldsymbol{e}_h^n\|^2\\ &\quad + \|\boldsymbol{u}^n\|_{L^\infty}\|\nabla\boldsymbol{\eta}^n\|^2 + \|\nabla\boldsymbol{\eta}^n\|_{L^\infty}\|\boldsymbol{\eta}^n\|^2\\ &\le C(\|\boldsymbol{\eta}^n\|_{L^2}^2 + \|\nabla\boldsymbol{\eta}^n\|_{L^2}^2 + \|\boldsymbol{e}_h^n\|_{L^2}^2),\end{aligned}$$

where we use $c(\boldsymbol{u}_h^n,\boldsymbol{e}_h^n,\boldsymbol{e}_h^n)=0$. By applying Hölder's inequality, the inverse inequality (8) and Young's inequality, we have

$$\begin{aligned}\Theta_{22} &= c(\boldsymbol{u}^n,\boldsymbol{u}^n,\boldsymbol{e}_h^{n+1}-\boldsymbol{e}_h^n) - c(\boldsymbol{u}_h^n,\boldsymbol{u}_h^n,\boldsymbol{e}_h^{n+1}-\boldsymbol{e}_h^n)\\ &= c(\boldsymbol{u}^n-\boldsymbol{u}_h^n,\boldsymbol{u}^n,\boldsymbol{e}_h^{n+1}-\boldsymbol{e}_h^n) + c(\boldsymbol{u}_h^n,\boldsymbol{u}^n-\boldsymbol{u}_h^n,\boldsymbol{e}_h^{n+1}-\boldsymbol{e}_h^n)\\ &= c(\boldsymbol{u}^n-\boldsymbol{u}_h^n,\boldsymbol{u}^n,\boldsymbol{e}_h^{n+1}-\boldsymbol{e}_h^n) + c(\boldsymbol{u}_h^n,\boldsymbol{\eta}^n,\boldsymbol{e}_h^{n+1}-\boldsymbol{e}_h^n) - c(\boldsymbol{u}_h^n,\boldsymbol{e}_h^n,\boldsymbol{e}_h^{n+1}-\boldsymbol{e}_h^n)\\ &\le \Big(1+\frac{\Delta t\|\boldsymbol{u}_h^n\|_{L^\infty}^2}{h^2}\Big)\frac{\|\boldsymbol{e}_h^{n+1}-\boldsymbol{e}_h^n\|_{L^2}^2}{64\Delta t} + C\Delta t\|\boldsymbol{\eta}^n\|_{L^2}^2 + Ch^2\|\nabla\boldsymbol{\eta}^n\|_{L^2}^2\\ &\qquad + C(\Delta t+1)\|\boldsymbol{e}_h^n\|_{L^2}^2.\end{aligned}$$

Now, we assume that for $0\le n\le N$,

$$\Delta t \le \frac{4h^2}{\|\boldsymbol{u}_h^n\|_{L^\infty}^2}. \tag{42}$$

At the end of the proof, we will verify the reasonableness of (42). With the restriction condition on the time step (42), we have

$$\Theta_2 \le \frac{5\|\boldsymbol{e}_h^{n+1}-\boldsymbol{e}_h^n\|_{L^2}^2}{64\Delta t} + C(\|\boldsymbol{\eta}^n\|_{L^2}^2 + \|\nabla\boldsymbol{\eta}^n\|_{L^2}^2 + \|\boldsymbol{e}_h^n\|_{L^2}^2).$$

Combining the above estimates, we can obtain

(43)

$$\begin{aligned}&c(\boldsymbol{u}^{n+1},\boldsymbol{u}^{n+1},\boldsymbol{e}_h^{n+1}) - \frac{q^{n+1}}{\exp(-\frac{t^{n+1}}{T})}c(\boldsymbol{u}_h^n,\boldsymbol{u}_h^n,\boldsymbol{e}_h^{n+1})\\ &\le\frac{3\|\boldsymbol{e}_h^{n+1}-\boldsymbol{e}_h^n\|_{L^2}^2}{16\Delta t} + C(\|\boldsymbol{\eta}^n\|_{L^2}^2+\|\nabla\boldsymbol{\eta}^n\|_{L^2}^2+\|\boldsymbol{e}_h^n\|_{L^2}^2+\Delta t\|\partial_t\boldsymbol{u}\|_{L^2(t^n,t^{n+1};\boldsymbol{H}^1(\Omega))}^2)+\Theta_3.\end{aligned}$$

Step 3. Next, we give an error estimate for the scalar auxiliary variable. We notice that the last term on the right-hand side of (43) can't be easily bounded, while it can be balanced with a term from (49).

Firstly, subtracting (18) from (16) leads to

$$\begin{aligned}&\frac{e_q^{n+1}-e_q^n}{\Delta t} + \frac{1}{T}e_q^{n+1}\\ =&\frac{-1}{\exp(-\frac{t^{n+1}}{T})}(c(\boldsymbol{u}_h^n,\boldsymbol{u}_h^n,\boldsymbol{u}_h^{n+1}) - c(\boldsymbol{u}^{n+1},\boldsymbol{u}^{n+1},\boldsymbol{u}^{n+1})) + \boldsymbol{E}_q^{n+1},\end{aligned} \tag{44}$$

with $\boldsymbol{E}_q^{n+1} = \frac{q(t^{n+1})-q(t^n)}{\Delta t} - q_t(t^{n+1})$. Multiplying both sides of (44) by e_q^{n+1} yields

$$
\begin{aligned}
&\frac{|e_q^{n+1}|^2 - |e_q^n|^2}{2\Delta t} + \frac{|e_q^{n+1} - e_q^n|^2}{2\Delta t} + \frac{1}{T}|e_q^{n+1}|^2 \\
=&\frac{-e_q^{n+1}}{\exp(-\frac{t^{n+1}}{T})}(c(\boldsymbol{u}_h^n, \boldsymbol{u}_h^n, e_h^{n+1}) - c(\boldsymbol{u}_h^n, \boldsymbol{u}_h^n, \boldsymbol{\eta}^{n+1}) \\
&- c(\boldsymbol{u}_h^n, \boldsymbol{u}^{n+1} - \boldsymbol{u}_h^n, \boldsymbol{u}^{n+1}) - c(\boldsymbol{u}^{n+1} - \boldsymbol{u}_h^n, \boldsymbol{u}^{n+1}, \boldsymbol{u}^{n+1})) + \boldsymbol{E}_q^{n+1} e_q^{n+1} \\
=&\frac{-e_q^{n+1}}{\exp(-\frac{t^{n+1}}{T})} c(\boldsymbol{u}_h^n, \boldsymbol{u}_h^n, e_h^{n+1}) + \frac{e_q^{n+1}}{\exp(-\frac{t^{n+1}}{T})} c(\boldsymbol{u}_h^n, \boldsymbol{u}_h^n, \boldsymbol{\eta}^{n+1}) \\
&+ \frac{e_q^{n+1}}{\exp(-\frac{t^{n+1}}{T})} c(\boldsymbol{u}_h^n, \boldsymbol{u}^{n+1} - \boldsymbol{u}_h^n, \boldsymbol{u}^{n+1}) + \boldsymbol{E}_q^{n+1} e_q^{n+1},
\end{aligned}
\tag{45}
$$

where we use $c(\boldsymbol{u}^{n+1} - \boldsymbol{u}_h^n, \boldsymbol{u}^{n+1}, \boldsymbol{u}^{n+1}) = 0$. Using $\boldsymbol{u}_h^n = \boldsymbol{e}_h^n + \boldsymbol{u}^n - \boldsymbol{\eta}^n$, the second term on the right-hand side of (45) can be bounded by

$$
\begin{aligned}
&\frac{e_q^{n+1}}{\exp(-\frac{t^{n+1}}{T})} c(\boldsymbol{u}_h^n, \boldsymbol{u}_h^n, \boldsymbol{\eta}^{n+1}) \\
=&\frac{e_q^{n+1}}{\exp(-\frac{t^{n+1}}{T})}(c(\boldsymbol{u}_h^n, \boldsymbol{u}^n, \boldsymbol{\eta}^{n+1}) + c(\boldsymbol{u}_h^n, \boldsymbol{e}_h^n, \boldsymbol{\eta}^{n+1}) - c(\boldsymbol{u}_h^n, \boldsymbol{\eta}^n, \boldsymbol{\eta}^{n+1})) \\
=&\frac{e_q^{n+1}}{\exp(-\frac{t^{n+1}}{T})}(c(\boldsymbol{u}_h^n, \boldsymbol{u}^n, \boldsymbol{\eta}^{n+1}) - c(\boldsymbol{u}_h^n, \boldsymbol{\eta}^{n+1}, \boldsymbol{e}_h^n) - c(\boldsymbol{u}_h^n, \boldsymbol{\eta}^n, \boldsymbol{\eta}^{n+1})) \\
\leq&C|e_q^{n+1}|\|\boldsymbol{u}_h^n\|\|\nabla \boldsymbol{u}^n\|_{L^\infty}\|\boldsymbol{\eta}^{n+1}\| + C|e_q^{n+1}|\|\boldsymbol{u}_h^n\|\|\boldsymbol{e}_h^n\|\|\nabla \boldsymbol{\eta}^{n+1}\|_{L^\infty} \\
&+ C|e_q^{n+1}|\|\boldsymbol{u}_h^n\|\|\boldsymbol{\eta}^{n+1}\|\|\nabla \boldsymbol{\eta}^n\|_{L^\infty} \\
\leq&\frac{1}{4T}|e_q^{n+1}|^2 + C\|\boldsymbol{e}_h^n\|^2 + C\|\boldsymbol{\eta}^{n+1}\|^2.
\end{aligned}
\tag{46}
$$

The third term on the right-hand side of (45) can be bounded by

$$
\begin{aligned}
&\frac{e_q^{n+1}}{\exp(-\frac{t^{n+1}}{T})} c(\boldsymbol{u}_h^n, \boldsymbol{u}^{n+1} - \boldsymbol{u}_h^n, \boldsymbol{u}^{n+1}) \\
\leq&C\|\boldsymbol{u}_h^n\|\|\boldsymbol{u}^{n+1} - \boldsymbol{u}_h^n\|\|\nabla \boldsymbol{u}^{n+1}\|_{L^\infty}|e_q^{n+1}| \\
\leq&\frac{1}{4T}|e_q^{n+1}|^2 + C\|\boldsymbol{e}_h^n\|^2 + C\|\boldsymbol{\eta}^n\|^2 + C\Delta t\|\partial_t \boldsymbol{u}\|^2_{L^2(t^n,t^{n+1};\boldsymbol{L}^2(\Omega))}.
\end{aligned}
\tag{47}
$$

For the last term on the right-hand side of (45), we have

$$
\boldsymbol{E}_q^{n+1} e_q^{n+1} \leq \frac{1}{4T}|e_q^{n+1}|^2 + C\Delta t\|q_{tt}\|^2_{L^2(t^n,t^{n+1})}.
\tag{48}
$$

By combining (46)-(48), we can obtain

$$
\begin{aligned}
&\frac{|e_q^{n+1}|^2 - |e_q^n|^2}{2\Delta t} + \frac{|e_q^{n+1} - e_q^n|^2}{2\Delta t} + \frac{1}{4T}|e_q^{n+1}|^2 \\
\leq&\frac{-e_q^{n+1}}{\exp(-\frac{t^{n+1}}{T})} c(\boldsymbol{u}_h^n, \boldsymbol{u}_h^n, e_h^{n+1}) + C(\|\boldsymbol{e}_h^n\|^2 + C\|\boldsymbol{\eta}^n\|^2 + C\|\boldsymbol{\eta}^{n+1}\|^2 \\
&+ \Delta t\|\partial_t \boldsymbol{u}\|^2_{L^2(t^n,t^{n+1};\boldsymbol{L}^2(\Omega))} + \Delta t\|q_{tt}\|^2_{L^2(t^n,t^{n+1})}).
\end{aligned}
\tag{49}
$$

Notice that we can use the first term on the right-hand side of (49) to balance the last term on the right-hand side of (43).

Step 4. Next, we can conclude (32) with the a priori assumption (42). To the end, we combine (35) and (49), and use (36), (38) and (43) to obtain

$$\begin{aligned}
&\frac{1}{2\Delta t}\|\boldsymbol{e}_h^{n+1}\|_{L^2}^2 + \frac{|e_q^{n+1}|^2}{2\Delta t} + \nu|\boldsymbol{e}_h^{n+1}|_1^2 \\
&\le \frac{1}{2\Delta t}\|\boldsymbol{e}_h^{n}\|_{L^2}^2 + \frac{|e_q^{n}|^2}{2\Delta t} + C\Big\{\|\partial_t\boldsymbol{\eta}^{n+1}\|_{L^2}^2 + \|\boldsymbol{\eta}^{n}\|_{L^2}^2 + \|\boldsymbol{\eta}^{n+1}\|_{L^2}^2 + \|\nabla\boldsymbol{\eta}^{n}\|_{L^2}^2 \\
&\quad + \Delta t\|\partial_{tt}\boldsymbol{u}\|_{L^2(t^n,t^{n+1};\boldsymbol{H}^1(\Omega))}^2 + \Delta t\|\partial_{t}\boldsymbol{u}\|_{L^2(t^n,t^{n+1};\boldsymbol{H}^1(\Omega))}^2 + \Delta t\|q_{tt}\|_{L^2(t^n,t^{n+1})}^2\Big\} \\
&\quad + C\|\boldsymbol{e}_h^{n}\|_{L^2}^2.
\end{aligned}$$

Summing over all discrete times, and by $\|\boldsymbol{e}_h^0\|_{L^2}^2 = 0$ and $|e_q^0|^2 = 0$, we can get

$$\|\boldsymbol{e}_h^{n+1}\|_{L^2}^2 + |e_q^{n+1}|^2 + \nu\Delta t\sum_{j=1}^{n+1}|\boldsymbol{e}_h^{j}|_1^2 \le C\Delta t\sum_{j=1}^{n+1}G_j + \Delta t\sum_{j=1}^{n+1}C\|\boldsymbol{e}_h^{j-1}\|_{L^2}^2,$$

with

$$\begin{aligned}
G_j &= \|\partial_t\boldsymbol{\eta}^{j}\|_{L^2}^2 + \|\boldsymbol{\eta}^{j-1}\|_{L^2}^2 + \|\boldsymbol{\eta}^{j}\|_{L^2}^2 + \|\nabla\boldsymbol{\eta}^{j-1}\|_{L^2}^2 \\
&\quad + \Delta t\|\partial_{tt}\boldsymbol{u}\|_{L^2(t^{j-1},t^j;\boldsymbol{H}^1(\Omega))}^2 + \Delta t\|\partial_{t}\boldsymbol{u}\|_{L^2(t^{j-1},t^j;\boldsymbol{H}^1(\Omega))}^2 + \Delta t\|q_{tt}\|_{L^2(t^{j-1},t^j)}^2.
\end{aligned}$$

Thus, the discrete Gronwall Lemma 2.1 can be applied, and one gets

$$\|\boldsymbol{e}_h^{n+1}\|_{L^2}^2 + |e_q^{n+1}|^2 + \nu\Delta t\sum_{j=1}^{n+1}|\boldsymbol{e}_h^{j}|_1^2 \le \exp(CT)(C\Delta t\sum_{j=1}^{n+1}G_j). \tag{50}$$

The application of the triangle inequality gives

$$\begin{aligned}
&\|\boldsymbol{u}^{n+1} - \boldsymbol{u}_h^{n+1}\|_{L^2}^2 + |e_q^{n+1}|^2 + \nu\Delta t\sum_{j=1}^{n+1}|\boldsymbol{u}^j - \boldsymbol{u}_h^j|_1^2 \\
&\le 2\|\boldsymbol{\eta}^{n+1}\|_{L^2}^2 + 2\nu\Delta t\sum_{j=1}^{n+1}|\boldsymbol{\eta}^j|_1^2 + \exp(CT)(C\Delta t\sum_{j=1}^{n+1}G_j).
\end{aligned}$$

Then, by using (10) and (13), we can conclude (32) with the a priori assumption (42). So, before we complete the proof, we need to verify the reasonableness of (42).

Step 5. Finally, we can check that due to (31), the a priori assumption (42) always holds for small enough h. To the end, we will prove that for small enough h, it holds that

$$\|\boldsymbol{u}_h^n\|_{L^\infty} \le 2\|\boldsymbol{u}\|_{L^\infty(0,T;\boldsymbol{L}^\infty(\Omega))}, \tag{51}$$

for $0 \le n \le N$, so that the CFL condition (31) implies (42).

First, there exists h_1 such that if $h \le h_1$, the right-hand sides of (10) and (11) are bounded by $\frac{3}{8C_{\text{inv}}}h^{\frac{d}{2}}\|\boldsymbol{u}\|_{L^\infty(0,T;\boldsymbol{L}^\infty(\Omega))}$ and $\frac{1}{4}\|\boldsymbol{u}\|_{L^\infty(0,T;\boldsymbol{L}^\infty(\Omega))}$, respectively. Furthermore, by the triangle inequality, we have

$$\|\boldsymbol{\pi}_s\boldsymbol{u}\|_{L^\infty(0,T;\boldsymbol{L}^\infty(\Omega))} \le \frac{5}{4}\|\boldsymbol{u}\|_{L^\infty(0,T;\boldsymbol{L}^\infty(\Omega))}.$$

Then, due to (31), there exists $h_2 < h_1$ such that if $h \le h_2$, the right-hand side of (32) is bounded by $\frac{9h^d}{64C_{\text{inv}}^2}\|\boldsymbol{u}\|_{L^\infty(0,T;\boldsymbol{L}^\infty(\Omega))}^2$.

Now, we prove (51) by mathematical induction. For $h \leq h_2$, (51) holds for $n = 0$ with $\boldsymbol{u}_h^0 = \boldsymbol{\pi}_s \boldsymbol{u}_0$. Supposing (51) holds for $n \leq m$, we can show that this assumption is also true for $n = m + 1$. Indeed, if (51) holds for $n \leq m$, then (32) holds for $n = m$. By using the inverse inequality (8), for $h \leq h_2$, we have

$$\begin{aligned}
\|\boldsymbol{u}_h^{m+1}\|_{L^\infty} &\leq \|\boldsymbol{u}_h^{m+1} - \boldsymbol{\pi}_s \boldsymbol{u}^{m+1}\|_{L^\infty} + \|\boldsymbol{\pi}_s \boldsymbol{u}^{m+1}\|_{L^\infty} \\
&\leq C_{\text{inv}} h^{-d/2} \|\boldsymbol{u}_h^{m+1} - \boldsymbol{\pi}_s \boldsymbol{u}^{m+1}\| + \|\boldsymbol{\pi}_s \boldsymbol{u}^{m+1}\|_{L^\infty} \\
&\leq C_{\text{inv}} h^{-d/2} \|\boldsymbol{u}^{m+1} - \boldsymbol{u}_h^{m+1}\| + C_{\text{inv}} h^{-d/2} \|\boldsymbol{u}^{m+1} - \boldsymbol{\pi}_s \boldsymbol{u}^{m+1}\| \\
&\quad + \frac{5}{4} \|\boldsymbol{u}\|_{L^\infty(0,T;\boldsymbol{L}^\infty(\Omega))} \\
&\leq 2\|\boldsymbol{u}\|_{L^\infty(0,T;\boldsymbol{L}^\infty(\Omega))}.
\end{aligned}$$

Consequently, (51) also holds for $n = m+1$. Thus, we have completed the proof. □

Remark 4.2. In the above proof, we first conclude (32) with the a priori assumption (42). Then, at the end of the proof, we verify the reasonableness of (42). Furthermore, to check the effectiveness of (42), we use the inverse inequality $\|\boldsymbol{u}_h^n\|_{L^\infty} \leq C_{\text{inv}} h^{-\frac{d}{2}} \|\boldsymbol{u}_h^n\|$ to obtain

$$\frac{h^{d+2}}{C_{\text{inv}}^2 \|\boldsymbol{u}_h^n\|^2} \leq \frac{h^2}{\|\boldsymbol{u}_h^n\|_{L^\infty}^2}.$$

Thus, it will be more convenient to compute the value of $\frac{h^{d+2}}{\|\boldsymbol{u}_h^n\|^2}$ at each time step in the following numerical experiments.

Next, based on the above analysis framework, we present the error analysis with error bounds obtained with no time step restrictions for the two-dimensional case, which is similar to that in [19]. It is proved that a Reynolds-dependent error bound $O(h^{k+1} + \Delta t)$ for the velocity L^2 error is obtained with no time step restrictions. Notice that for the SAV scheme combined with the FEM [27], the velocity L^2 error is only suboptimal with convergence order of k in space.

Theorem 4.3. *Let $\Omega \subset \mathbb{R}^2$, $\boldsymbol{u}_h^0 = \boldsymbol{\pi}_s \boldsymbol{u}_0$ and $q^0 = 1$, and assume the regularities (30) of the velocity solution. Then, we have the following error estimates: for $0 \leq n \leq N$,*

$$\|\boldsymbol{u}^{n+1} - \boldsymbol{u}_h^{n+1}\|_{L^2}^2 + |e_q^{n+1}|^2 \leq C(\boldsymbol{u}, \partial_t \boldsymbol{u}, \partial_{tt} \boldsymbol{u}, T, \nu^{-1})(h^{2k+2} + (\Delta t)^2),$$
$$\nu \Delta t \sum_{j=1}^{n+1} |\boldsymbol{u}^j - \boldsymbol{u}_h^j|_1^2 \leq C(\boldsymbol{u}, \partial_t \boldsymbol{u}, \partial_{tt} \boldsymbol{u}, T, \nu^{-1})(h^{2k} + (\Delta t)^2),$$

with a constant $C(\boldsymbol{u}, \partial_t \boldsymbol{u}, \partial_{tt} \boldsymbol{u}, T, \nu^{-1})$ independent of n and h.

Proof. The proof follows that of Theorem 4.1 with the changes that we will comment on. Notice that much of our previous analysis can be reused for the new error bounds, except for the handling of the nonlinear term Θ_2.

For Θ_{21}, we have

$$\begin{aligned}
\Theta_{21} &= c(\boldsymbol{\eta}^n, \boldsymbol{u}^n, \boldsymbol{e}_h^n) - c(\boldsymbol{e}_h^n, \boldsymbol{u}^n, \boldsymbol{e}_h^n) + c(\boldsymbol{e}_h^n, \boldsymbol{\eta}^n, \boldsymbol{e}_h^n) + c(\boldsymbol{u}^n, \boldsymbol{\eta}^n, \boldsymbol{e}_h^n) - c(\boldsymbol{\eta}^n, \boldsymbol{\eta}^n, \boldsymbol{e}_h^n) \\
&\leq \|\nabla \boldsymbol{u}^n\|_{L^\infty}\|\boldsymbol{\eta}^n\|^2 + 2\|\nabla \boldsymbol{u}^n\|_{L^\infty}\|\boldsymbol{e}_h^n\|^2 + 2\|\nabla \boldsymbol{\eta}^n\|_{L^\infty}\|\boldsymbol{e}_h^n\|^2 + \frac{1}{8}\nu\|\nabla \boldsymbol{e}_h^n\|^2 \\
&\quad + \frac{2}{\nu}\|\boldsymbol{u}^n\|_{L^\infty}^2\|\boldsymbol{\eta}^n\|^2 + \|\nabla \boldsymbol{\eta}^n\|_{L^\infty}\|\boldsymbol{\eta}^n\|^2 \\
&\leq C(\|\boldsymbol{\eta}^n\|_{L^2}^2 + \frac{1}{\nu}\|\boldsymbol{\eta}^n\|^2 + \|\boldsymbol{e}_h^n\|_{L^2}^2) + \frac{1}{8}\nu\|\nabla \boldsymbol{e}_h^n\|^2,
\end{aligned}$$

where only the handling of the term $c(\boldsymbol{u}^n, \boldsymbol{\eta}^n, \boldsymbol{e}_h^n)$ is different from that of (41). By writing $\boldsymbol{u}_h^n = \boldsymbol{e}_h^n + \boldsymbol{u}^n - \boldsymbol{\eta}^n$, we have

$$\begin{aligned}
\Theta_{22} &= c(\boldsymbol{u}^n - \boldsymbol{u}_h^n, \boldsymbol{u}^n, \boldsymbol{e}_h^{n+1} - \boldsymbol{e}_h^n) + c(\boldsymbol{u}_h^n, \boldsymbol{u}^n - \boldsymbol{u}_h^n, \boldsymbol{e}_h^{n+1} - \boldsymbol{e}_h^n) \\
&= c(\boldsymbol{u}^n - \boldsymbol{u}_h^n, \boldsymbol{u}^n, \boldsymbol{e}_h^{n+1} - \boldsymbol{e}_h^n) - c(\boldsymbol{u}^n, \boldsymbol{e}_h^{n+1} - \boldsymbol{e}_h^n, \boldsymbol{\eta}^n) + c(\boldsymbol{e}_h^n, \boldsymbol{\eta}^n, \boldsymbol{e}_h^{n+1} - \boldsymbol{e}_h^n) \\
&\quad - c(\boldsymbol{\eta}^n, \boldsymbol{\eta}^n, \boldsymbol{e}_h^{n+1} - \boldsymbol{e}_h^n) - \underbrace{c(\boldsymbol{u}_h^n, \boldsymbol{e}_h^n, \boldsymbol{e}_h^{n+1} - \boldsymbol{e}_h^n)}_{\Theta_{221}} \\
&\leq \frac{\|\boldsymbol{e}_h^{n+1} - \boldsymbol{e}_h^n\|_{L^2}^2}{32\Delta t} + C\Delta t\|\nabla \boldsymbol{u}^n\|_{L^\infty}^2\|\boldsymbol{\eta}^n\|_{L^2}^2 + C\Delta t\|\nabla \boldsymbol{u}^n\|_{L^\infty}^2\|\boldsymbol{e}_h^n\|_{L^2}^2 \\
&\quad + C\frac{1}{\nu}\|\boldsymbol{u}^n\|_{L^\infty}^2\|\boldsymbol{\eta}^n\|_{L^2}^2 + \frac{1}{8}\nu\|\nabla \boldsymbol{e}_h^{n+1}\|_{L^2}^2 + \frac{1}{8}\nu\|\nabla \boldsymbol{e}_h^n\|_{L^2}^2 \\
&\quad + C\Delta t\|\nabla \boldsymbol{\eta}^n\|_{L^\infty}^2\|\boldsymbol{\eta}^n\|_{L^2}^2 + C\Delta t\|\nabla \boldsymbol{\eta}^n\|_{L^\infty}^2\|\boldsymbol{e}_h^n\|_{L^2}^2 - \Theta_{221}.
\end{aligned}$$

For the term Θ_{221}, by writing $\boldsymbol{u}_h^n = \boldsymbol{e}_h^n + \boldsymbol{u}^n - \boldsymbol{\eta}^n$, and using (4), (10) and the inverse inequality (8), we can obtain

$$\begin{aligned}
\Theta_{221} &= c(\boldsymbol{u}^n, \boldsymbol{e}_h^n, \boldsymbol{e}_h^{n+1} - \boldsymbol{e}_h^n) + c(\boldsymbol{e}_h^n, \boldsymbol{e}_h^n, \boldsymbol{e}_h^{n+1} - \boldsymbol{e}_h^n) - c(\boldsymbol{\eta}^n, \boldsymbol{e}_h^n, \boldsymbol{e}_h^{n+1} - \boldsymbol{e}_h^n) \\
&= -c(\boldsymbol{u}^n, \boldsymbol{e}_h^{n+1}, \boldsymbol{e}_h^n) - c(\boldsymbol{e}_h^n, \boldsymbol{e}_h^{n+1}, \boldsymbol{e}_h^n) + c(\boldsymbol{\eta}^n, \boldsymbol{e}_h^{n+1}, \boldsymbol{e}_h^n) \\
&\leq \|\boldsymbol{u}^n\|_{L^\infty}\|\nabla \boldsymbol{e}_h^{n+1}\|_{L^2}\|\boldsymbol{e}_h^n\|_{L^2} + C\|\boldsymbol{e}_h^n\|_{L^2}{}^{\frac{1}{2}}\|\nabla \boldsymbol{e}_h^n\|_{L^2}{}^{\frac{1}{2}}\|\nabla \boldsymbol{e}_h^{n+1}\|_{L^2}\|\boldsymbol{e}_h^n\|_{L^2}{}^{\frac{1}{2}}\|\nabla \boldsymbol{e}_h^n\|_{L^2}{}^{\frac{1}{2}} \\
&\quad + C\|\boldsymbol{\eta}^n\|_{L^2}{}^{\frac{1}{2}}\|\nabla \boldsymbol{\eta}^n\|_{L^2}{}^{\frac{1}{2}}\|\nabla \boldsymbol{e}_h^{n+1}\|_{L^2}\|\boldsymbol{e}_h^n\|_{L^2}{}^{\frac{1}{2}}\|\nabla \boldsymbol{e}_h^n\|_{L^2}{}^{\frac{1}{2}} \\
&\leq \|\boldsymbol{u}^n\|_{L^\infty}\|\nabla \boldsymbol{e}_h^{n+1}\|_{L^2}\|\boldsymbol{e}_h^n\|_{L^2} + C\|\boldsymbol{e}_h^n\|_{L^2}\|\nabla \boldsymbol{e}_h^n\|_{L^2}\|\nabla \boldsymbol{e}_h^{n+1}\|_{L^2} \\
&\quad + C\|\nabla \boldsymbol{u}^n\|_{L^2}\|\nabla \boldsymbol{e}_h^{n+1}\|_{L^2}\|\boldsymbol{e}_h^n\|_{L^2} \\
&\leq \frac{C}{\nu}(1 + \|\nabla \boldsymbol{u}_h^n\|_{L^2}^2)\|\boldsymbol{e}_h^n\|_{L^2}^2 + \frac{1}{8}\nu\|\nabla \boldsymbol{e}_h^{n+1}\|_{L^2}^2,
\end{aligned}$$

where we use the classical embedding inequality $\|\nabla \boldsymbol{u}^n\|_{L^2} \leq C\|\nabla \boldsymbol{u}^n\|_{L^\infty}$. With no time step restrictions, we can obtain

$$\begin{aligned}
\Theta_2 \leq \frac{\|\boldsymbol{e}_h^{n+1} - \boldsymbol{e}_h^n\|_{L^2}^2}{32\Delta t} &+ C(1 + \frac{1}{\nu})\|\boldsymbol{\eta}^n\|_{L^2}^2 + \frac{1}{4}\nu\|\nabla \boldsymbol{e}_h^n\|_{L^2}^2 + \frac{1}{4}\nu\|\nabla \boldsymbol{e}_h^{n+1}\|_{L^2}^2 \\
&+ C(1 + \frac{1}{\nu})\|\boldsymbol{e}_h^n\|_{L^2}^2 + \frac{C}{\nu}\|\nabla \boldsymbol{u}_h^n\|_{L^2}^2\|\boldsymbol{e}_h^n\|_{L^2}^2.
\end{aligned}$$

Then, following Steps 1-4 of the proof of Theorem 4.1, we can conclude the proof. Notice that when the discrete Gronwall lemma is applied, the stability estimate $\Delta t \sum_{j=1}^{n+1} \|\nabla \boldsymbol{u}_h^j\|_{L^2}^2 \leq \frac{C}{\nu}$ from (22) will be used. ◻

Remark 4.4. Notice that the estimate of Θ_{221} is only limited to the case of $d = 2$. For the three-dimensional case, we have

$$\Theta_{221} = c(\boldsymbol{u}_h^n, \boldsymbol{e}_h^n, \boldsymbol{e}_h^{n+1} - \boldsymbol{e}_h^n) \leq \frac{\|\boldsymbol{e}_h^{n+1} - \boldsymbol{e}_h^n\|_{L^2}^2}{16\Delta t} + \frac{4\Delta t}{\nu}\|\boldsymbol{u}_h^n\|_{L^\infty}^2 \nu \|\nabla \boldsymbol{e}_h^n\|_{L^2}^2.$$

As before, we first assume that for $0 \leq n \leq N$,

$$\frac{\Delta t}{\nu}\|\boldsymbol{u}_h^n\|_{L^\infty}^2 \leq \frac{1}{16}. \tag{52}$$

We can show that for small enough h, (52) always holds with the time step constraint

$$\Delta t \leq \min\{\frac{\nu}{64\|\boldsymbol{u}\|_{L^\infty(0,T;\boldsymbol{L}^\infty(\Omega))}^2}, h^{\frac{3}{2}+\epsilon}\}(\epsilon > 0). \tag{53}$$

Arguing as in Step 5 of the proof of Theorem 4.1, it is easily proved that for small enough h, we have

$$\|\boldsymbol{u}_h^n\|_{L^\infty} \leq 2\|\boldsymbol{u}\|_{L^\infty(0,T;\boldsymbol{L}^\infty(\Omega))}.$$

Thus, (52) will be a consequence of (53). So, with the time step constraint (53), the similar error estimates can be also obtained for the three-dimensional case.

Remark 4.5. Here, for the two-dimensional case, the Reynolds-dependent error estimates don't require any time step constraint, as in [19], but for the three-dimensional case, the error estimates are obtained with the time step constraint (53). Notice that for the SAV pressure-correction scheme, the error analysis does not require any time-step constraint, which is only limited to the two-dimensional case. For the three-dimensional case, it has some technical difficulties, see [19]. For the three-dimensional case, error estimates obtained without any time step constraint will be our future research direction.

5. Numerical studies

In this section, we present some numerical examples to check our analytical results, which were implemented in the NGSolve software [23]. We use the Scott-Vogelius pair with $k = 2$ in Example 5.1 and Example 5.2, and $k = 4$ in Example 5.3. For applying the Scott-Vogelius pair with $k = 2$, we use a sequence of the unstructured regular and quasi-uniform triangulations with mesh size $h = 1/M$, then an additional barycentric refinement of the triangulations was applied to guarantee the satisfaction of the discrete inf-sup condition. For $k = 4$, we use a general shape-regular mesh without the additional barycentric refinement [13].

Example 5.1. In this example, we test an analytical solution with a small value of ν to check the effectiveness of the CFL condition. Furthermore, the optimal and suboptimal convergence rates in space are observed for large and small values of ν, respectively.

Let the domain $\Omega = (0, 1)^2$ and choose the exact solutions of (1) [7] given by

$$\boldsymbol{u}(x, y, t) = \frac{6 + 4\cos(4t)}{10}\begin{bmatrix} 8\sin^2(\pi x)(2y(1-y)(1-2y)) \\ -8\pi\sin(2\pi x)(y(1-y))^2 \end{bmatrix},$$

$$p(x, y, t) = \frac{6 + 4\cos(4t)}{10}\sin(\pi x)\cos(\pi y).$$

We take the small viscosity $\nu = 10^{-8}$, and the final time $T = 1.6$. We use the above-mentioned mesh with $M = 10$ to observe the variation of the errors with respect to Δt. For temporal discretization, to compare the IMEX-SAV scheme, we use the semi-implicit and IMEX schemes without the SAV, in which $c(\boldsymbol{u}_h^n, \boldsymbol{u}_h^{n+1}, \boldsymbol{v}_h)$ and $c(\boldsymbol{u}_h^n, \boldsymbol{u}_h^n, \boldsymbol{v}_h)$ are used as the discrete convection terms, respectively. From Table 1, we can observe that the IMEX scheme is conditionally energy stable and has the matched errors, which are comparable to that of the semi-implicit scheme. The semi-implicit scheme is better in the respect that there is almost no restriction on the time step. The IMEX-SAV scheme is unconditionally energy stable, however conditionally has the matched errors with restriction on the time step. These are consistent with our theoretical results.

We can compute the value of $\Delta t_n = \frac{h^4}{\|\boldsymbol{u}_h^n\|_{L^2}^2}$ (see Remark 4.2) at each time step. From Figure 1, we can observe that whenever the actual time step Δt (solid line) is smaller than the computed time steps (dotted line), or whenever the actual time step is close to the minimum value of the computed time steps, the IMEX-SAV method has the matched errors, in which the errors are comparable to that of the semi-implicit scheme, see the actual time step $\Delta t = \frac{1}{320}, \frac{1}{640}, \frac{1}{1280}, \frac{1}{2560}$ in Figure 1 and Table 1. On the contrary, the IMEX-SAV method hasn't the matched errors, see the actual time step $\Delta t = \frac{1}{20}, \frac{1}{40}, \frac{1}{80}, \frac{1}{160}$ in Figure 1 and Table 1.

TABLE 1. Behavior of errors for the IMEX, IMEX-SAV and semi-implicit schemes with respect to the time step

Δt	$\|\boldsymbol{u}_h\|_{L^2}$	$\|\boldsymbol{u}-\boldsymbol{u}_h\|_{L^2}$	$\|\nabla(\boldsymbol{u}-\boldsymbol{u}_h)\|_{L^2}$	$\|p-p_h\|_{L^2}$	$\|\nabla\cdot\boldsymbol{u}_h\|_{L^2}$	$\lvert q(T)-q^{N+1}\rvert$
IMEX						
$\frac{1}{20}$	nan	nan	nan	nan	nan	—
$\frac{1}{40}$	nan	nan	nan	nan	nan	—
$\frac{1}{80}$	nan	nan	nan	nan	nan	—
$\frac{1}{160}$	1.85e+00	1.63e+00	1.26e+02	3.42e+00	2.02e-14	—
$\frac{1}{320}$	9.69e-01	8.52e-02	7.30e+00	5.77e-02	8.12e-15	—
$\frac{1}{640}$	9.68e-01	6.87e-02	5.58e+00	4.07e-02	1.55e-14	—
$\frac{1}{1280}$	9.68e-01	6.79e-02	5.51e+00	3.98e-02	5.63e-15	—
$\frac{1}{2560}$	9.68e-01	6.76e-02	5.48e+00	3.95e-02	3.62e-15	—
IMEX-SAV						
$\frac{1}{20}$	1.14e+00	6.18e-01	4.67e+01	6.93e-01	7.50e-15	3.68e-01
$\frac{1}{40}$	1.16e+00	6.58e-01	4.86e+01	6.84e-01	1.68e-14	3.62e-01
$\frac{1}{80}$	1.07e+00	5.26e-01	3.66e+01	6.86e-01	5.80e-15	3.63e-01
$\frac{1}{160}$	1.02e+00	3.28e-01	2.83e+01	6.28e-01	4.13e-15	3.32e-01
$\frac{1}{320}$	9.69e-01	8.50e-02	7.26e+00	5.95e-02	5.45e-15	5.39e-03
$\frac{1}{640}$	9.68e-01	6.87e-02	5.58e+00	4.07e-02	2.88e-15	4.22e-05
$\frac{1}{1280}$	9.68e-01	6.79e-02	5.51e+00	3.98e-02	2.53e-14	2.38e-05
$\frac{1}{2560}$	9.68e-01	6.76e-02	5.48e+00	3.95e-02	1.23e-14	1.67e-05
Semi-Implicit						
$\frac{1}{20}$	9.63e-01	6.19e-02	5.06e+00	3.50e-02	6.26e-15	—
$\frac{1}{40}$	9.57e-01	6.50e-02	5.32e+00	3.68e-02	4.41e-15	—
$\frac{1}{80}$	9.63e-01	6.54e-02	5.35e+00	3.76e-02	2.87e-15	—
$\frac{1}{160}$	9.67e-01	6.57e-02	5.35e+00	3.81e-02	2.91e-15	—
$\frac{1}{320}$	9.68e-01	6.64e-02	5.40e+00	3.86e-02	2.94e-15	—
$\frac{1}{640}$	9.67e-01	6.69e-02	5.44e+00	3.90e-02	9.89e-15	—
$\frac{1}{1280}$	9.68e-01	6.71e-02	5.45e+00	3.91e-02	3.15e-14	—
$\frac{1}{2560}$	9.68e-01	6.72e-02	5.46e+00	3.92e-02	2.73e-15	—

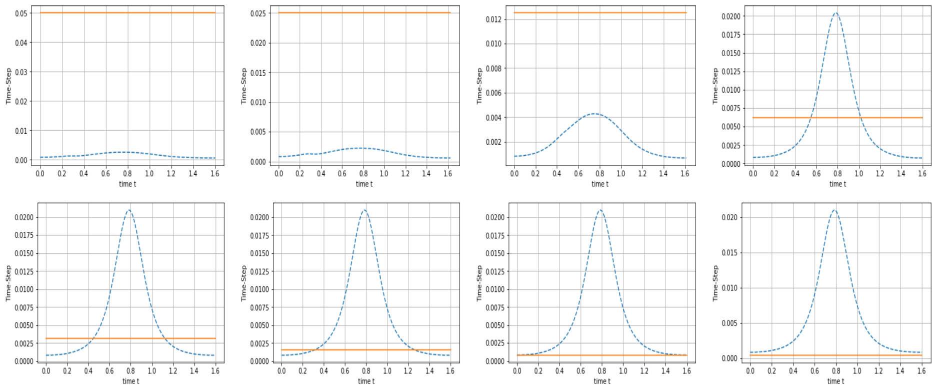

FIGURE 1. Time evolution of the computed time steps (dotted line) and actual time step (solid line), from left to right: $\Delta t = \frac{1}{20}$, $\frac{1}{40}$, $\frac{1}{80}$, $\frac{1}{160}$ (see first row) and $\Delta t = \frac{1}{320}$, $\frac{1}{640}$, $\frac{1}{1280}$, $\frac{1}{2560}$ (see second row)

Furthermore, we can give the first-order IMEX-SAV-Adaptation (ISA) scheme, which can be written as follows: find $(\boldsymbol{u}_h^{n+1}, p_h^{n+1}, q^{n+1})$ such that for $\forall(\boldsymbol{v}_h, q_h) \in \boldsymbol{V}_h \times Q_h$,

$$(\frac{\boldsymbol{u}_h^{n+1} - \boldsymbol{u}_h^n}{\Delta t_n}, \boldsymbol{v}_h) + \nu a(\boldsymbol{u}_h^{n+1}, \boldsymbol{v}_h) + b(\boldsymbol{v}_h, p_h^{n+1}) + \frac{q^{n+1}}{\exp(-\frac{t^{n+1}}{T})} c(\boldsymbol{u}_h^n, \boldsymbol{u}_h^n, \boldsymbol{v}_h) = (\boldsymbol{f}^{n+1}, \boldsymbol{v}_h),$$

$$b(\boldsymbol{u}_h^{n+1}, q_h) = 0,$$

and

$$\frac{q^{n+1} - q^n}{\Delta t_n} = -\frac{1}{T} q^{n+1} + \frac{1}{\exp(-\frac{t^{n+1}}{T})} c(\boldsymbol{u}_h^n, \boldsymbol{u}_h^n, \boldsymbol{u}_h^{n+1}),$$

with the adaptive time step $\Delta t_n = \frac{h^4}{\|\boldsymbol{u}_h^n\|_{L^2}^2}$(here, $t^{n+1} = t^n + \Delta t_n$).

TABLE 2. Errors of the IMEX-SAV-Adaptation and semi-implicit schemes with the adaptive time step Δt_n and the mesh with $M = 10$

	Δt	$\|\boldsymbol{u}_h\|_{L^2}$	$\|\boldsymbol{u} - \boldsymbol{u}_h\|_{L^2}$	$\|\nabla(\boldsymbol{u} - \boldsymbol{u}_h)\|_{L^2}$	$\|p - p_h\|_{L^2}$	$\|\nabla \cdot \boldsymbol{u}_h\|_{L^2}$	$\lvert q(T) - q^{N+1}\rvert$
Semi-Implicit	Δt_n	9.84e-01	6.76e-02	5.59e+00	4.17e-02	7.76e-15	–
ISA	Δt_n	9.84e-01	6.99e-02	5.80e+00	4.58e-02	5.13e-14	3.15e-04

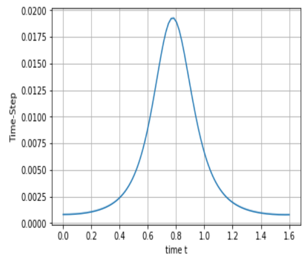

FIGURE 2. Time evolution of the adaptive time step

For the semi-implicit scheme, we use the same time-step size as that of the ISA scheme. From Table 2, we can observe that the errors of the ISA scheme are comparable to that of the semi-implicit scheme. From Figure 2, we can see the time evolution of adaptive time step.

Next, we test the convergence rates of the velocity, pressure and scalar auxiliary variable errors. As for temporal discretization, the IMEX-SAV scheme was applied. We set the time step small enough to ensure that the spatial error dominates over the temporal error. We take the small time step $\triangle t = 0.1(1/M)^3$. The above-mentioned meshes are used with $M = 4, 8, 16, 32$. From Table 3, the velocity, pressure and scalar auxiliary variable errors have the error bounds, as predicted by the theoretical estimates in Theorems 4.1 and A.1. With the same settings, for large value of ν, $\nu = 10^{-1}$, the optimal convergence rates in space for the velocity L^2 errors can be observed from Table 4.

TABLE 3. Errors and convergence rates with the IMEX-SAV scheme (17)-(18) with $\nu = 10^{-8}$

M	$\|\boldsymbol{u} - \boldsymbol{u}_h\|_{L^2}$	Rate	$\|p - p_h\|_{L^2(0,T;L^2(\Omega))}$	Rate	$\lvert q(T) - q^{N+1}\rvert$	Rate
4	1.56e-01	–	7.56e-02	–	4.61e-04	–
8	4.35e-02	1.84	1.46e-02	2.37	2.01e-05	4.52
16	1.11e-02	1.97	2.67e-03	2.45	2.68e-06	2.91
32	2.87e-03	1.96	5.60e-04	2.25	3.79e-07	2.82

TABLE 4. Errors and convergence rates with the IMEX-SAV scheme (17)-(18) with $\nu = 10^{-1}$

M	$\|\boldsymbol{u} - \boldsymbol{u}_h\|_{L^2}$	Rate	$\|p - p_h\|_{L^2(0,T;L^2(\Omega))}$	Rate	$\lvert q(T) - q^{N+1}\rvert$	Rate
4	7.14e-02	–	3.04e-01	–	1.75e-04	–
8	6.26e-03	3.51	6.63e-02	2.20	2.24e-05	2.97
16	6.23e-04	3.33	1.52e-02	2.12	2.81e-06	2.99
32	8.37e-05	2.90	3.74e-03	2.02	3.51e-07	3.00

Example 5.2. Here, we test whether the error estimates are obtained with no time step restrictions for a larger value of the viscosity. To this end, we test a numerical example in [19] to see if similar results can be obtained.

We consider the following exact solution of (1) on the domain $\Omega = (0,1)^2$:

$$\boldsymbol{u}(x,y,t) = \begin{bmatrix} \sin(t)\sin^2(\pi x)\sin(2\pi y) \\ -\sin(t)\sin(2\pi x)\sin^2(\pi y) \end{bmatrix},$$
$$p(x,y,t) = \sin(t)(\sin(\pi y) - 2/\pi).$$

We set $T = 1$ and $\nu = 0.1$. The above-mentioned mesh is used with $M = 230$, which can ensure that the temporal discretization error is dominant over the spatial discretization error.

We test the convergence rates for the first-order and second-order IMEX-SAV schemes, respectively. The second-order IMEX-SAV scheme can be written as follows: find $(\boldsymbol{u}_h^{n+1}, p_h^{n+1}, q^{n+1})$ such that for $\forall(\boldsymbol{v}_h, q_h) \in \boldsymbol{V}_h \times Q_h$,

(54)
$$\left(\frac{3\boldsymbol{u}_h^{n+1} - 4\boldsymbol{u}_h^n + \boldsymbol{u}_h^{n-1}}{2\Delta t}, \boldsymbol{v}_h\right) + \nu a(\boldsymbol{u}_h^{n+1}, \boldsymbol{v}_h) + b(\boldsymbol{v}_h, p_h^{n+1}) + \frac{q^{n+1}}{\exp(-\frac{t^{n+1}}{T})} c(\hat{\boldsymbol{u}}_h^n, \hat{\boldsymbol{u}}_h^n, \boldsymbol{v}_h) = F(\boldsymbol{v}_h),$$
$$b(\boldsymbol{u}_h^{n+1}, q_h) = 0,$$

and

$$\frac{3q^{n+1} - 4q^n + q^{n-1}}{2\Delta t} = -\frac{1}{T}q^{n+1} + \frac{1}{\exp(-\frac{t^{n+1}}{T})} c(\hat{\boldsymbol{u}}_h^n, \hat{\boldsymbol{u}}_h^n, \boldsymbol{u}_h^{n+1}), \tag{55}$$

with $\hat{\boldsymbol{u}}_h^n = 2\boldsymbol{u}_h^n - \boldsymbol{u}_h^{n-1}$ and $F(\boldsymbol{v}_h) = (\boldsymbol{f}^{n+1}, \boldsymbol{v}_h)$. Here, we use the first-order IMEX-SAV scheme in the first time step.

The first-order convergence rates in time for the velocity, pressure and SAV errors are observed in Table 5. The second-order convergence rates for the velocity and SAV errors, and nearly second-order convergence rate for the pressure errors are observed in Table 6. These are basically consistent with the results in [19].

TABLE 5. Errors and convergence rates with the first-order IMEX-SAV scheme (17)-(18)

Δt	$\|\boldsymbol{u} - \boldsymbol{u}_h\|_{L^2}$	Rate	$\|p - p_h\|_{L^2(0,T;L^2(\Omega))}$	Rate	$\|q(T) - q^{N+1}\|$	Rate
$\frac{1}{10}$	4.39e-03	–	2.13e-02	–	1.76e-02	–
$\frac{1}{20}$	2.08e-03	1.08	1.02e-02	1.06	9.01e-03	0.97
$\frac{1}{40}$	1.04e-03	1.00	5.11e-03	1.00	4.55e-03	0.99
$\frac{1}{80}$	5.25e-04	0.99	2.57e-03	0.99	2.29e-03	0.99

TABLE 6. Errors and convergence rates with the second-order IMEX-SAV scheme (54)-(55)

Δt	$\|\boldsymbol{u} - \boldsymbol{u}_h\|_{L^2}$	Rate	$\|p - p_h\|_{L^2(0,T;L^2(\Omega))}$	Rate	$\|q(T) - q^{N+1}\|$	Rate
$\frac{1}{10}$	2.94e-04	–	3.11e-03	–	1.39e-03	–
$\frac{1}{20}$	8.81e-05	1.74	6.32e-04	2.30	3.97e-04	1.81
$\frac{1}{40}$	1.88e-05	2.23	1.59e-04	1.99	9.74e-05	2.03
$\frac{1}{80}$	5.03e-06	1.89	4.73e-05	1.75	2.36e-05	2.05

Example 5.3. In this test case, we test a classical benchmark problem, where a laminar flow around a cylinder is considered [17, 22].

The domain Ω is a rectangular channel, $[0, 2.2] \times [0, 0.41]$ with a circular obstacle of radius $r = 0.05$, which is centered at $(0.2, 0.2)$ within the channel. The boundary $\partial\Omega$ is decomposed into $\Gamma_{out} := \{x = 2.2\}$, the outflow boundary, $\Gamma_{in} := \{x = 0\}$, the inflow boundary, and $\Gamma_{wall} := \partial\Omega \backslash (\Gamma_{in} \cup \Gamma_{out})$, the wall boundary. On Γ_{in}, we prescribe the Dirichlet boundary condition

$$\boldsymbol{u}(0, y, t) = \frac{1}{0.41^2} \begin{bmatrix} 6y(0.41 - y) \\ 0 \end{bmatrix}.$$

On Γ_{out}, we prescribe the homogeneous Neumann boundary condition $(-\nu\nabla\boldsymbol{u} + pI)\boldsymbol{n} = 0$. The homogeneous Dirichlet boundary condition for the velocity is imposed on Γ_{wall}. The viscosity is set as $\nu = 10^{-3}$.

We use a (curved) unstructured triangular mesh around the cylinder, in which the mesh consists of 1368 cells with mesh size $h \approx 0.04$ away from the cylinder, and $h \approx 0.01$ around the cylinder, see Figure 3. Notice that we use the Scott-Vogelius pair with $k = 4$, which allows us to use a general mesh without the additional barycentric refinement. For the temporal discretization, the second-order IMEX-SAV scheme is applied with $\Delta t = 3 \times 10^{-5}$. First, we start a simulation with an initial velocity, which is computed by solving the steady Stokes solution of this problem. Then, the computed velocity solution at $t = 1$ is saved and this solution will be used as the initial velocity at $t = 0$ for the following simulation, see Figure 3. The final time of the following simulation is taken to be $T = 8$.

Notice that in the implementation, to deal with the complex boundary conditions, the discrete convection term in (55) should be replaced by $c_{skew}(\hat{\boldsymbol{u}}_h^n, \hat{\boldsymbol{u}}_h^n, \boldsymbol{u}_h^{n+1}) = \frac{1}{2}c(\hat{\boldsymbol{u}}_h^n, \hat{\boldsymbol{u}}_h^n, \boldsymbol{u}_h^{n+1}) - \frac{1}{2}c(\hat{\boldsymbol{u}}_h^n, \boldsymbol{u}_h^{n+1}, \hat{\boldsymbol{u}}_h^n)$ such that in a continuous sense, $c_{skew}(\boldsymbol{u}, \boldsymbol{u}, \boldsymbol{u}) = 0$, with the exact solution $\boldsymbol{u}$ of this problem.

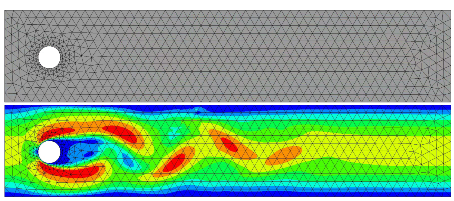

FIGURE 3. Sketch of the mesh and the initial velocity magnitude (color corresponding to velocity magnitude from 0 to 2.133)

Quantities of interest in Example 5.3 are the drag and lift coefficients at the cylinder. At each time step, we compute the drag and lift coefficients, which are defined as [15]

$$\begin{aligned} c_{\text{drag}} &= -20((d_t\boldsymbol{u}_h^n, \boldsymbol{e}_x) + \nu a(\boldsymbol{u}_h^n, \boldsymbol{e}_x) + b(\boldsymbol{e}_x, p_h^n) + c(\boldsymbol{u}_h^n, \boldsymbol{u}_h^n, \boldsymbol{e}_x)), \\ c_{\text{lift}} &= -20((d_t\boldsymbol{u}_h^n, \boldsymbol{e}_y) + \nu a(\boldsymbol{u}_h^n, \boldsymbol{e}_y) + b(\boldsymbol{e}_y, p_h^n) + c(\boldsymbol{u}_h^n, \boldsymbol{u}_h^n, \boldsymbol{e}_y)), \end{aligned}$$

where $d_t\boldsymbol{u}_h^n = \frac{3\boldsymbol{u}_h^n - 4\boldsymbol{u}_h^{n-1} + \boldsymbol{u}_h^{n-2}}{2\Delta t}$, when $n > 1$, $d_t\boldsymbol{u}_h^n = \frac{\boldsymbol{u}_h^n - \boldsymbol{u}_h^{n-1}}{\Delta t}$, when $n = 1$. Here, $\boldsymbol{e}_x$ and $\boldsymbol{e}_y$ are continuous piecewise quartic functions taking values $\boldsymbol{e}_x = [1, 0]^T$ and $\boldsymbol{e}_y = [0, 1]^T$ on those nodes on the surface of the cylinder, respectively, and vanishing on all the other nodes. We compute the maximum and minimum drag coefficients, $\max c_{\text{drag}} = 3.22795$ and $\min c_{\text{drag}} = 3.16468$, respectively, and the maximum and minimum lift coefficients, $\max c_{\text{lift}} = 0.98786$ and $\min c_{\text{lift}} = -1.02273$, respectively, which are comparable to the results in the literature [17,22]. In Figure 4, the velocity magnitude at $T = 8$ is shown.

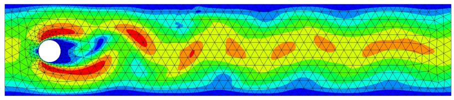

FIGURE 4. The velocity magnitude of flow around a cylinder at $T = 8$ (color corresponding to velocity magnitude from 0 to 2.209)

APPENDIX A. ERROR ANALYSIS FOR THE PRESSURE

In this appendix, we present the error analysis for the pressure. First, we make the error splitting, as follows:

$$p^n - p_h^n = (p^n - P^{k-1}p^n) - (p_h^n - P^{k-1}p^n) = \eta_p^n - e_p^n,$$

where $P^{k-1}p^n$ denotes the L^2-projection of p^n onto Q_h.

Theorem A.1. *Under the assumptions of Theorem 4.1, we have the following error estimate:*

$$\begin{aligned}
&\Delta t \sum_{n=1}^{N+1} \|p^n - p_h^n\|_{L^2}^2 \\
&\le C(1 + h^{-1})\big\{T \max_{1\le n\le N+1} (\|\boldsymbol{u}^{n-1} - \boldsymbol{u}_h^{n-1}\|^2 + |e_q^n|^2) + \|\eta_p\|^2_{\mathcal{L}^2(0,t^{N+1};L^2(\Omega))} \\
&\quad + \nu^2 \Delta t \sum_{n=1}^{N+1} |\boldsymbol{u}^n - \boldsymbol{u}_h^n|_1^2 + \|\partial_t \boldsymbol{\eta}\|^2_{\mathcal{L}^2(0,t^{N+1};\boldsymbol{L}^2(\Omega))} + (\Delta t)^2 \|\partial_{tt}\boldsymbol{u}\|^2_{L^2(0,t^{N+1};\boldsymbol{H}^1(\Omega))} \\
&\quad + (\Delta t)^2 \|\partial_t \boldsymbol{u}\|^2_{L^2(0,t^{N+1};\boldsymbol{L}^2(\Omega))}\big\},
\end{aligned}$$

with a constant C independent of h and ν^{-1}.

Proof. Notice that much of the analysis is very similar to that of [7,8], so we only concentrate on what is really different, mainly the nonlinear terms and the scalar auxiliary variable. We can refer to [7,8] for more details.

First, we have the following error equation

(56)
$$\begin{aligned}
&b(\boldsymbol{v}_h, e_p^{n+1}) \\
&= b(\boldsymbol{v}_h, \eta_p^{n+1}) + (\partial_t(\boldsymbol{u}^{n+1} - \boldsymbol{\pi}_s\boldsymbol{u}^{n+1}), \boldsymbol{v}_h) + (\partial_t \boldsymbol{\pi}_s \boldsymbol{u}^{n+1} - \frac{\boldsymbol{\pi}_s\boldsymbol{u}^{n+1} - \boldsymbol{\pi}_s\boldsymbol{u}^n}{\Delta t}, \boldsymbol{v}_h) \\
&\quad - (D_t \boldsymbol{e}_h^{n+1}, \boldsymbol{v}_h) + \nu a(\boldsymbol{u}^{n+1} - \boldsymbol{u}_h^{n+1}, \boldsymbol{v}_h) \\
&\quad + \underbrace{\frac{q(t^{n+1})}{\exp(-\frac{t^{n+1}}{T})} c(\boldsymbol{u}^{n+1}, \boldsymbol{u}^{n+1}, \boldsymbol{v}_h) - \frac{q^{n+1}}{\exp(-\frac{t^{n+1}}{T})} c(\boldsymbol{u}_h^n, \boldsymbol{u}_h^n, \boldsymbol{v}_h)}_{\phi},
\end{aligned}$$

with $D_t\boldsymbol{e}_h^{n+1} = \frac{\boldsymbol{e}_h^{n+1}-\boldsymbol{e}_h^n}{\Delta t}$. Denote

$$\phi = \underbrace{c(\boldsymbol{u}^n,\boldsymbol{u}^n,\boldsymbol{v}_h) - \frac{q^{n+1}}{\exp(-\frac{t^{n+1}}{T})}c(\boldsymbol{u}_h^n,\boldsymbol{u}_h^n,\boldsymbol{v}_h)}_{\phi_1} + \underbrace{c(\boldsymbol{u}^{n+1}-\boldsymbol{u}^n,\boldsymbol{u}^{n+1},\boldsymbol{v}_h) + c(\boldsymbol{u}^n,\boldsymbol{u}^{n+1}-\boldsymbol{u}^n,\boldsymbol{v}_h)}_{\phi_2}.$$

By using Hölder's inequality, we have

$$\begin{aligned}\phi_1 =& c(\boldsymbol{u}^n,\boldsymbol{u}^n,\boldsymbol{v}_h) - \frac{q^{n+1}}{\exp(-\frac{t^{n+1}}{T})}c(\boldsymbol{u}_h^n,\boldsymbol{u}_h^n,\boldsymbol{v}_h)\\ =& \frac{q^{n+1}}{\exp(-\frac{t^{n+1}}{T})}c(\boldsymbol{u}^n-\boldsymbol{u}_h^n,\boldsymbol{u}^n,\boldsymbol{v}_h) + \frac{q^{n+1}}{\exp(-\frac{t^{n+1}}{T})}c(\boldsymbol{u}_h^n,\boldsymbol{u}^n-\boldsymbol{u}_h^n,\boldsymbol{v}_h)\\ &+ \frac{e_q^{n+1}}{\exp(-\frac{t^{n+1}}{T})}c(\boldsymbol{u}^n,\boldsymbol{u}^n,\boldsymbol{v}_h)\\ \le& C(\|\boldsymbol{u}^n-\boldsymbol{u}_h^n\| + |e_q^{n+1}|)\|\nabla\boldsymbol{v}_h\|,\end{aligned}$$

where we use $\|\boldsymbol{u}_h^n\|_{L^\infty(\Omega)} \le C$ from (51) and $|q^n| \le c_1, \forall 0 \le n \le N+1$. Similarly, we have

$$\begin{aligned}\phi_2 &= -c(\boldsymbol{u}^{n+1}-\boldsymbol{u}^n,\boldsymbol{v}_h,\boldsymbol{u}^{n+1}) - c(\boldsymbol{u}^n,\boldsymbol{v}_h,\boldsymbol{u}^{n+1}-\boldsymbol{u}^n)\\ &\le C(\Delta t)^{\frac12}\|\partial_t\boldsymbol{u}\|_{L^2(t^n,t^{n+1};\boldsymbol{L}^2(\Omega))}\|\nabla\boldsymbol{v}_h\|_{L^2}.\end{aligned}$$

Then, the above estimates are combined to obtain

$$\phi \le C(\|\boldsymbol{u}^n-\boldsymbol{u}_h^n\| + |e_q^{n+1}| + (\Delta t)^{\frac12}\|\partial_t\boldsymbol{u}\|_{L^2(t^n,t^{n+1};\boldsymbol{L}^2(\Omega))})\|\nabla\boldsymbol{v}_h\|. \tag{57}$$

We take the test function $\boldsymbol{v}_h = (A_h)^{-1}D_t\boldsymbol{e}_h^{n+1} \in \boldsymbol{V}_h^{\mathrm{div}}$ in (56), and use (57) and (5) to obtain

$$\begin{aligned}\|D_t\boldsymbol{e}_h^{n+1}\|_{-1} &\le Ch^{-\frac12}\|(A_h)^{-\frac12}D_t\boldsymbol{e}_h^{n+1}\|\\ &\le Ch^{-\frac12}\big\{\nu|\boldsymbol{u}^{n+1}-\boldsymbol{u}_h^{n+1}|_1 + (\|\boldsymbol{u}^n-\boldsymbol{u}_h^n\| + |e_q^{n+1}|\\ &\quad + (\Delta t)^{\frac12}\|\partial_t\boldsymbol{u}\|_{L^2(t^n,t^{n+1};\boldsymbol{L}^2(\Omega))})\\ &\quad + \|\partial_t\boldsymbol{\eta}^{n+1}\|_{L^2} + \|\partial_t\boldsymbol{\pi}_s\boldsymbol{u}^{n+1} - \frac{\boldsymbol{\pi}_s\boldsymbol{u}^{n+1}-\boldsymbol{\pi}_s\boldsymbol{u}^n}{\Delta t}\|_{L^2}\big\},\end{aligned} \tag{58}$$

where we use (3) in [8], (5) and the inverse inequality (8) to get the first inequality. Applying the discrete inf-sup condition (3), (57) and (58), we can obtain

$$
\begin{aligned}
\beta\|e_p^{n+1}\|_{L^2} \leq & \sup_{\boldsymbol{v}_h \in \boldsymbol{V}_h \setminus 0} \frac{b(\boldsymbol{v}_h, e_p^{n+1})}{|\boldsymbol{v}_h|_1} \\
\leq & C\big\{\|D_t \boldsymbol{e}_h^{n+1}\|_{-1} + \|\eta_p^{n+1}\|_{L^2} + \nu|\boldsymbol{u}^{n+1} - \boldsymbol{u}_h^{n+1}|_1 + \|\partial_t \boldsymbol{\pi}_s \boldsymbol{u}^{n+1} \\
& - \frac{\boldsymbol{\pi}_s \boldsymbol{u}^{n+1} - \boldsymbol{\pi}_s \boldsymbol{u}^n}{\Delta t}\| + (\|\boldsymbol{u}^n - \boldsymbol{u}_h^n\| + |e_q^{n+1}| \\
& + (\Delta t)^{\frac{1}{2}} \|\partial_t \boldsymbol{u}\|_{L^2(t^n, t^{n+1}; \boldsymbol{L}^2(\Omega))}) + \|\partial_t \boldsymbol{\eta}^{n+1}\|_{L^2}\big\} \\
\leq & C(1 + h^{-\frac{1}{2}})\big\{\|\eta_p^{n+1}\|_{L^2} + \nu|\boldsymbol{u}^{n+1} - \boldsymbol{u}_h^{n+1}|_1 \\
& + (\Delta t)^{\frac{1}{2}} \|\partial_{tt} \boldsymbol{u}\|_{L^2(t^n, t^{n+1}; \boldsymbol{H}^1(\Omega))} + (\|\boldsymbol{u}^n - \boldsymbol{u}_h^n\| + |e_q^{n+1}| \\
& + (\Delta t)^{\frac{1}{2}} \|\partial_t \boldsymbol{u}\|_{L^2(t^n, t^{n+1}; \boldsymbol{L}^2(\Omega))}) + \|\partial_t \boldsymbol{\eta}^{n+1}\|_{L^2}\big\}.
\end{aligned}
$$

Finally, by applying the triangle inequality, we can conclude the proof. □

Remark A.2. By combining Theorem A.1 and (32), we can obtain

$$
(\Delta t \sum_{n=1}^{N+1} \|p^n - p_h^n\|_{L^2}^2)^{\frac{1}{2}} \leq C(\boldsymbol{u}, \partial_t \boldsymbol{u}, \partial_{tt} \boldsymbol{u}, p, T)(1 + h^{-\frac{1}{2}})(h^k + \Delta t).
$$

This kind of error bound can be seen in [8].

References

[1] R. A. Adams and J. J. F. Fournier, *Sobolev Spaces*, 2nd ed., Pure and Applied Mathematics (Amsterdam), vol. 140, Elsevier/Academic Press, Amsterdam, 2003. MR2424078

[2] N. Ahmed, G. R. Barrenechea, E. Burman, J. Guzmán, A. Linke, and C. Merdon, *A pressure-robust discretization of Oseen's equation using stabilization in the vorticity equation*, SIAM J. Numer. Anal. **59** (2021), no. 5, 2746–2774, DOI 10.1137/20M1351230. MR4331937

[3] F. Boyer and P. Fabrie, *Mathematical Tools for the Study of the Incompressible Navier-Stokes Equations and Related Models*, Applied Mathematical Sciences, vol. 183, Springer, New York, 2013, DOI 10.1007/978-1-4614-5975-0. MR2986590

[4] S. C. Brenner and L. R. Scott, *The Mathematical Theory of Finite Element Methods*, 3rd ed., Texts in Applied Mathematics, vol. 15, Springer, New York, 2008, DOI 10.1007/978-0-387-75934-0. MR2373954

[5] H. Chen, *Pointwise error estimates for finite element solutions of the Stokes problem*, SIAM J. Numer. Anal. **44** (2006), no. 1, 1–28, DOI 10.1137/S0036142903438100. MR2217368

[6] P. G. Ciarlet, *The Finite Element Method for Elliptic Problems*, Classics in Applied Mathematics, vol. 40, Society for Industrial and Applied Mathematics (SIAM), Philadelphia, PA, 2002. Reprint of the 1978 original [North-Holland, Amsterdam; MR0520174 (58 #25001)], DOI 10.1137/1.9780898719208. MR1930132

[7] J. de Frutos, B. García-Archilla, and J. Novo, *Fully discrete approximations to the time-dependent Navier-Stokes equations with a projection method in time and grad-div stabilization*, J. Sci. Comput. **80** (2019), no. 2, 1330–1368, DOI 10.1007/s10915-019-00980-9. MR3977208

[8] J. de Frutos, B. García-Archilla, and J. Novo, *Corrigenda: Fully discrete approximations to the time-dependent Navier-Stokes equations with a projection method in time and grad-div stabilization*, J. Sci. Comput. **88** (2021), no. 2, Paper No. 40, 3, DOI 10.1007/s10915-021-01551-7. MR4280515

[9] V. DeCaria and M. Schneier, *An embedded variable step IMEX scheme for the incompressible Navier-Stokes equations*, Comput. Methods Appl. Mech. Engrg. **376** (2021), Paper No. 113661, 26, DOI 10.1016/j.cma.2020.113661. MR4198151

[10] A. Ern and J.-L. Guermond, *Theory and Practice of Finite Elements*, Applied Mathematical Sciences, vol. 159, Springer-Verlag, New York, 2004, DOI 10.1007/978-1-4757-4355-5. MR2050138

[11] B. García-Archilla, V. John, and J. Novo, *On the convergence order of the finite element error in the kinetic energy for high Reynolds number incompressible flows*, Comput. Methods Appl. Mech. Engrg. **385** (2021), Paper No. 114032, 54, DOI 10.1016/j.cma.2021.114032. MR4290202

[12] B. Garcia-Archilla and J. Novo, *Robust error bounds for the Navier-Stokes equations using implicit-explicit second order BDF method with variable steps*, Preprint, arXiv:2112.12446, 2021.

[13] J. Guzmán and L. R. Scott, *The Scott-Vogelius finite elements revisited*, Math. Comp. **88** (2019), no. 316, 515–529, DOI 10.1090/mcom/3346. MR3882274

[14] F. Huang and J. Shen, *Stability and error analysis of a class of high-order IMEX schemes for Navier-Stokes equations with periodic boundary conditions*, SIAM J. Numer. Anal. **59** (2021), no. 6, 2926–2954, DOI 10.1137/21M1404144. MR4342123

[15] V. John, *Finite Element Methods for Incompressible Flow Problems*, Springer Series in Computational Mathematics, vol. 51, Springer, Cham, 2016, DOI 10.1007/978-3-319-45750-5. MR3561143

[16] W. Layton, *Introduction to the numerical analysis of incompressible viscous flows*, Computational Science & Engineering, vol. 6, Society for Industrial and Applied Mathematics (SIAM), Philadelphia, PA, 2008. With a foreword by Max Gunzburger, DOI 10.1137/1.9780898718904. MR2442411

[17] C. Lehrenfeld and J. Schöberl, *High order exactly divergence-free hybrid discontinuous Galerkin methods for unsteady incompressible flows*, Comput. Methods Appl. Mech. Engrg. **307** (2016), 339–361, DOI 10.1016/j.cma.2016.04.025. MR3511719

[18] X. Li and J. Shen, *Error analysis of the SAV-MAC scheme for the Navier-Stokes equations*, SIAM J. Numer. Anal. **58** (2020), no. 5, 2465–2491, DOI 10.1137/19M1288267. MR4146381

[19] X. Li, J. Shen, and Z. Liu, *New SAV-pressure correction methods for the Navier-Stokes equations: stability and error analysis*, Math. Comp. **91** (2021), no. 333, 141–167, DOI 10.1090/mcom/3651. MR4350535

[20] L. Lin, Z. Yang, and S. Dong, *Numerical approximation of incompressible Navier-Stokes equations based on an auxiliary energy variable*, J. Comput. Phys. **388** (2019), 1–22, DOI 10.1016/j.jcp.2019.03.012. MR3933268

[21] H. Morgan and L. R. Scott, *Towards a unified finite element method for the Stokes equations*, SIAM J. Sci. Comput. **40** (2018), no. 1, A130–A141, DOI 10.1137/16M1103117. MR3746508

[22] M. Schäfer, S. Turek, F. Durst, E. Krause, and R. Rannacher, *Benchmark computations of laminar flow around a cylinder*, Flow Simulation with High-Performance Computers II, Springer, 1996, pp. 547–566.

[23] J. Schöberl, *C++ 11 implementation of finite elements in NGSolve*, No. 30,Institute for Analysis and Scientific Computing, Vienna University of Technology, 2014.

[24] P. W. Schroeder and G. Lube, *Pressure-robust analysis of divergence-free and conforming FEM for evolutionary incompressible Navier-Stokes flows*, J. Numer. Math. **25** (2017), no. 4, 249–276, DOI 10.1515/jnma-2016-1101. MR3767413

[25] L. R. Scott and M. Vogelius, *Norm estimates for a maximal right inverse of the divergence operator in spaces of piecewise polynomials* (English, with French summary), RAIRO Modél. Math. Anal. Numér. **19** (1985), no. 1, 111–143, DOI 10.1051/m2an/1985190101111. MR813691

[26] R. Temam, *Navier-Stokes Equations*, AMS Chelsea Publishing, Providence, RI, 2001. Theory and numerical analysis; Reprint of the 1984 edition, DOI 10.1090/chel/343. MR1846644

[27] T. Zhang and J. Yuan, *Unconditional stability and optimal error estimates of Euler implicit/explicit-SAV scheme for the Navier-Stokes equations*, J. Sci. Comput. **90** (2022), no. 1, Paper No. 1, 20, DOI 10.1007/s10915-021-01681-y. MR4342664

College of Science, Henan University of Technology, Zhengzhou, Henan 450001, People's Republic of China; and School of Mathematics and Statistics, Xi'an Jiaotong University, Xi'an, Shaanxi 710049, People's Republic of China

Email address: hyb204514@stu.xjtu.edu.cn

College of Mathematics and System Science, Xinjiang University, Wulumuqi 830046, People's Republic of China; and School of Mathematics and Statistics, Xi'an Jiaotong University, Xi'an, Shaanxi 710049, People's Republic of China

Email address: yrhou@mail.xjtu.edu.cn

School of Mathematics and Statistics, Xi'an Jiaotong University, Xi'an, Shaanxi 710049, People's Republic of China

Email address: 1287951827@qq.com